

DEVELOPMENT OF A HIGH POWER STABILIZED DIODE LASER SYSTEM

by

MATTHIAS FUCHS

A THESIS

Presented to the Department of Physics
and the Graduate School of the University of Oregon
in partial fulfillment of the requirements
for the degree of
Master of Science

June 2006

“DEVELOPMENT OF A HIGH POWER STABILIZED DIODE LASER SYSTEM,”
a thesis prepared by Matthias Fuchs in partial fulfillment of the requirements for the
Master of Science degree in the Department of Physics. This thesis has been approved
and accepted by:

Professor Daniel Steck, Chair of the Examining Committee

Date

Committee in charge: Professor Daniel Steck, Chair
 Professor Michael Raymer
 Professor Stehphen Gregory

Accepted by:

Vice Provost and Dean of the Graduate School

DEVELOPMENT OF A HIGH POWER STABILIZED DIODE LASER SYSTEM

Copyright June 2006

by

Matthias Fuchs

An Abstract of the Thesis of

Matthias Fuchs for the degree of Master of Science

in the Department of Physics to be taken June 2006

Title: DEVELOPMENT OF A HIGH POWER STABILIZED DIODE
LASER SYSTEM

Approved: _____
Professor Daniel Steck

This thesis describes the design and realization of a high power diode laser system. The system consists of a single mode external cavity diode laser (ECDL) which is injection locked into a free running laser diode. The beam of this low power master-slave configuration is coupled into a high power tapered amplifier diode. The goal of the laser system is to provide a dipole trap for ultra-cold Rubidium atoms. The output power of the system is 1 W.

DEDICATION

This is for my parents and for Matthias Baar, who left us long before his time.

ACKNOWLEDGEMENTS

Without all the help of my colleagues and friends, I could never have successfully finished the task that I'm describing in this thesis.

First of all I want to thank my adviser Dan Steck. He was always there when I needed advice, whether it was on theoretical concepts, experimental procedures or just a good idea to put drain pipe cleaner on food. He always took time to explain and to discuss physics problems. He invented the long, long tradition of the weekly Friday ice cream, which definitely contributed to the relaxed atmosphere in the lab. I also want to thank my lab mates for helping me and providing a fun working environment.

Tao Li was a great help to me in explaining some optics setup procedures. It was always fun and interesting to talk with him about Chinese culture and sports.

Libby Schoene added a female note to the lab and just by her presence made being in the lab a nicer experience. I always enjoyed discussing both physics and non-physics related subjects with her.

It was also a pleasure to bug Aaron Webster by any means possible. He is just the man to have weird conversations with and to tell funny stories. Jeremy Thorn always reminded me when it was "cookie time". He helped me greatly in writing a program that fetches data from the voltmeter. Otherwise, my measurements would have taken about a Zillion years. Jeremy and Aaron were also responsible for introducing me to some very instructive short movies about the Martians from Sesame Street.

Finally, I cannot forget Peter Gaskell who was always very helpful when I had problems with electronics or computers.

Overall, there is a very good working atmosphere in the Steck lab that made me get up every morning and willingly go to work. I am very confident that this lab and of course the people working in it have much potential and eventful, successful and bright futures.

Without the people working in the machine shop I could also never have built such a device. Kris, John and Jeff showed me how a lathe and a milling machine work, and even managed to teach me how to machine precise parts. They were all a big help when I needed suggestions on how to machine . . . basically anything.

I also want to thank Emelie. Without her, I probably would never have started this project. I want to thank her for all her love and all the wonderful time that we could spend together. She was there for me every day and helped me through the dark days full of frustration, but she was also there to share my joy. The walks with her often helped me to get my thoughts off of problems and to rejuvenate my mind and eventually solve the problems with fresh ideas. She is constant source of joy. Her endless will to bug me and her sense of humor infinitely brightened up my life.

Of course, I also want to thank my parents, my brother, and my friends back in Germany. Although we were spatially very far separated, we were very close in spirit. It is not an easy step to leave one's home to live in a foreign country, but all my friends and family supported me and helped me with my decision.

And then I came to the US ...and made more friends. They all helped me to have a good time here and even made me stay longer than I originally planned. I can definitely conclude that these two years in the US were among the best years of my live.

CURRICULUM VITA

NAME OF AUTHOR: Matthias Fuchs

PLACE OF BIRTH: Ellwangen, Germany

DATE OF BIRTH: August 6, 1980

GRADUATE AND UNDERGRADUATE SCHOOLS ATTENDED:

University of Oregon
Universität Stuttgart, Germany

DEGREES AWARDED:

Master of Science in Physics, 2006, University of Oregon
Vordiplom in physics, 2003 Universität Stuttgart

TABLE OF CONTENTS

Chapter	Page
I. INTRODUCTION	1
I.1. Dipole Trap	2
I.2. Quantum-Mechanical Description	3
II. THEORY OF THE LASER	8
II.1. Interaction of Photons and Atoms	8
II.2. Rate Equation	10
II.3. Elements of a Laser	11
II.4. The Principle of a Laser	13
II.5. The Diode Laser	14
II.6. Absorption and Emission Revisited	19
II.7. TE & TM Polarization	26
II.8. Current, Temperature and Frequency Dependence	28
II.9. The Tapered Amplifier	30
III. THE EXPERIMENTAL SETUP	36
III.1. The “Lasers” s	36
III.2. Pseudo-External-Cavity Laser or the “Master”	37
III.3. Frequency Stabilizing the Master Laser	38
III.4. Slave Laser	41
III.5. Optical Setup I	42
III.6. Injection Locking the Master to the Slave Laser	43
III.7. Injecting the Slave Laser in the Tapered Amplifier	46
III.8. Optical Setup II	47
III.9. Handling of the Tapered Amplifier	49
III.10. Design Considerations for the Housing of the TA	50
III.11. The Temperature Encounter	54
IV. Results	57
IV.1. Amplified Spontaneous Emission	57

IV.2. Amplification of the Seed Beam	59
IV.3. Spectrum	61
IV.4. Optimizing the Output of the TA	62
IV.5. Spatial Profile	63
V. Conclusions	68
APPENDIX	69
A. Technical Drawings	70
BIBLIOGRAPHY	72

List of Figures

Figure	Page
I.1 Blue (left) and red detuned (right) Gaussian laser beam that repel and attract atoms, respectively.	3
II.1 Gain curve of a laser with the modes of the resonator.	15
II.2 p-n junction with an external potential U	18
II.3 Cut through a p-i-n heterostructure energy diagram, size of electrons and holes not to scale.	20
II.4 One dimensional energy diagram for electrons and holes. E_c is the energy of the conduction band, E_v the energy of the valence band. An electron combines with a hole and a photon of energy $\hbar\omega$ is emitted.	21
II.5 Radiative transitions in semiconductors: a.) spontaneous emission, b.) stimulated emission and c.) stimulated absorption.	22
II.6 Energy diagram of a multi-quantum well surrounded by a confinement structure.	27
II.7 The peak emission wavelength of a diode laser. The dashed line represents the change of the peak gain and the solid line the changes of the cavity length and the refractive index. After [3].	29
II.8 Schematic drawing of a tapered amplifier.	30
II.9 Far-field intensity pattern of a tapered amplifier.	34
II.10 Picture of the tapered amplifier compared to a match. The golden colored part is the c-mount of the diode. The real diode is the small blue dot on top of the mount. It appears to be blue in this picture but it is black in reality.	35
III.1 Picture of the optical setup.	36
III.2 Picture of the master laser. The path of the laser beam is indicated by the red line.	37
III.3 Picture of the Slave Laser.	41
III.4 Schematic of the optical setup.	42
III.5 Tapered amplifier with the out-coupling optics to compensate for the astigmatism.	48
III.6 Sideview of the tapered amplifier housing.	51
III.7 Picture of the tapered amplifier housing.	53
III.8 Schematic of the protection circuit. The diodes prevent the TA from forward and backward transients, the ferrit bead and the capacitors form a low-pass filter. The ferrite beads ⁽¹⁾ are Panasonic EXC-ELSA 35.	54
III.9 Schematic drawing of the tapered amplifier housing.	55

IV.1	Horizontal beam profile of the amplified spontaneous emission at a current of $I_{TA} = 0.75A$, after the collimation and the cylindrical lens.	57
IV.2	Horizontal beam profile of the amplified spontaneous emission at a current of $I_{TA} = 0.75A$, after the collimation and the cylindrical lens.	58
IV.3	Low resolution ASE spectrum at $I_{TA} = 1.5A$ and $17.5\text{ }^\circ\text{C}$	59
IV.4	Power of the input laser versus the amplified power for two amplifier currents: 1600 mA and 2000 mA.	60
IV.5	Temperature dependence of the output power versus the driving current.	60
IV.6	Output power versus current for two different seed powers of 8 mW and 13 mW.	61
IV.7	Spectrum of the TA for a output power of 0.5 W. The solid curve is optimized for the most absolute power, the dashed curve for the most power at 780 nm. The inset shows the difference between both graphs. Note: the inset has a linear y-axis.	62
IV.8	Horizontal profile for a seeding laser power of $P_{seed} = 8\text{ mW}$ and an amplifier power of $P_{TA} = 100\text{ mW}$	64
IV.9	Vertical profile for a seeding laser power of $P_{seed} = 8\text{ mW}$ and an amplifier power of $P_{TA} = 100\text{ mW}$	65
IV.10	Horizontal profile of the TA for the same input power of 8 mW and an output power of the tapered amplifier of 100 mW and 400 mW.	65
IV.11	Vertical profile of the TA for the same input power of 8 mW and an output power of the tapered amplifier of 100 mW and 400 mW.	66
IV.12	Horizontal beam profile for different input powers at the same output power of 100 mW.	67
IV.13	Vertical beam profile for different input powers at the same output power of 100 mW.	67
V.1	Picture of the tapered amplifier, emitting to the left, with the two collimation lenses.	68
A.1	Drawing of the large copper block (A).	70
A.2	Drawing of the baseplate with water-cooling ability.	71

CHAPTER I

INTRODUCTION

In recent years, semiconductor diode lasers have shown improved reliability, power, and wavelength coverage. With the ability to provide more power, diode lasers can now compete with heavy and bulky gas and other solid-state lasers. They have become increasingly common in industrial applications, since they are compact, easy to cool, and have a power efficiency upwards of 50%. Another advantage of diode lasers is that they can have a very high spatial beam quality, and their frequency can be very easily and rapidly tuned by changing the injection current. Furthermore, with the development of the semiconductor industry, they have also become less expensive.

Concerning the work in science, diode lasers have become one of the workhorses for atomic physics. In order to confine ultra-cold rubidium atoms in a dipole trap, powerful lasers with a wavelength in the vicinity of 780 nm are often used. Atoms are scattered out of a dipole trap at a rate of $\Gamma_{\text{sc}} \sim I/\Delta^2$ with I being the intensity of the laser beam and Δ the detuning of the beam frequency from the atomic transition. Therefore a far detuning is needed. However, since the potential of the trap has a dependence of $U \sim I/\Delta$, a high intensity beam is also necessary.

I.1. Dipole Trap

First, a brief overview of the dipole trap is given. For a more in-depth description, refer to [1].

The dipole trap confines neutral atoms using the interaction of light with an atom. Light is nothing more than an electromagnetic field that exerts a force on an electric dipole moment. Since rubidium is a neutral atom, it possesses in the ground state no permanent electric dipole moment. But the field of a laser induces a shift on the energy states of an atom. This shift, known as the AC Stark shift or light shift, is a change of potential energy of the atom. Therefore, if the potential is lowered by the interaction with the light and the electromagnetic field of the laser is inhomogeneous (has a gradient), the atom moves to the place with the lowest potential, which is the spot with the highest field. Since the induced shift is not static but oscillatory, the frequency of the laser light also has to be taken into account. If the light is below the atomic resonance (red detuned), the energy of the ground state and therefore the potential is lowered, resulting in an attractive force towards the highest intensity of the field. On the other hand, if the light frequency is higher than the resonance frequency (blue detuned), the ground state is raised, which means that the atom is repelled by high intensities. This behavior can be understood by using the classical Lorentz model of an atom. In this model the atom consists of a very heavy core (compared to the electron) and an electron which is bound to the core via a spring

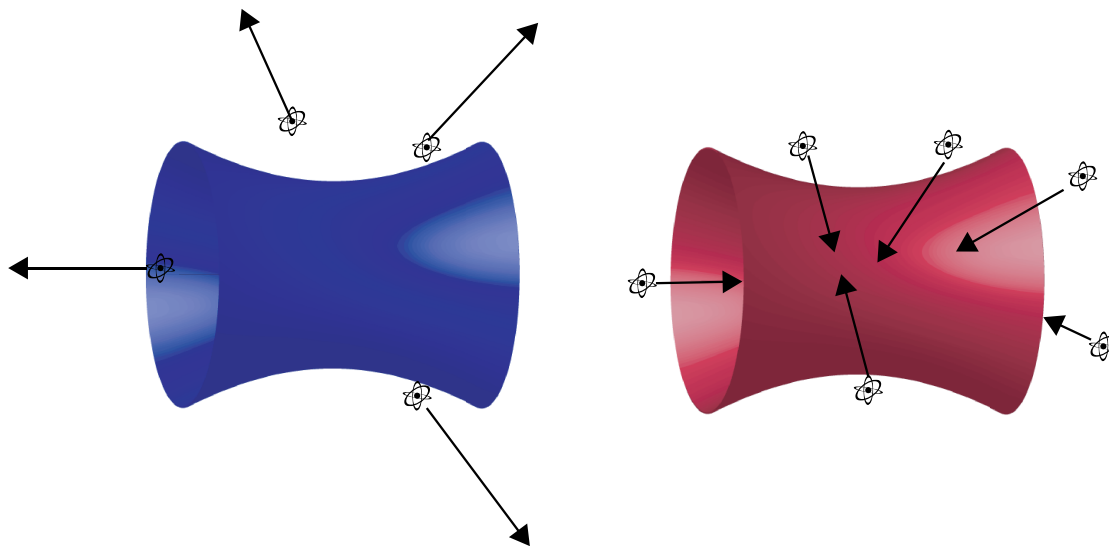


FIGURE I.1: Blue (left) and red detuned (right) Gaussian laser beam that repel and attract atoms, respectively.

representing the electromagnetic force. If this system is now driven by an external oscillator (the optical field) with a frequency below the resonance frequency, the system can “keep up” and stays in phase with the light field thus drawing the atom into the region where the oscillator is the strongest. If the oscillator frequency exceeds the resonance, the system can no longer follow and becomes out of phase, so that the dipole moment opposes the light field and the atom is repelled by high intensities.

I.2. Quantum-Mechanical Description

A quantum-mechanical formulation is now presented to give an overview of the mathematical description of the dipole trap.

The so-called “dressed-atom picture” describes the coupling of a two-level atom

with a light field. The Hamilton operator of such a system is the following:

$$\hat{H} = \hat{H}_A + \hat{H}_L + \hat{V}_{AL}. \quad (\text{I.1})$$

Here, \hat{H}_A is the Hamiltonian of the two level system with a ground state $|g\rangle$ and excited state $|e\rangle$, separated by an energy of $\hbar\omega_A$,

$$\hat{H}_A = \hbar\omega_A |e\rangle \langle e|, \quad (\text{I.2})$$

and \hat{H}_L is the Hamiltonian of the light field. For simplification, only a monochromatic field with a frequency ω_L is considered. By using the creation and annihilation operators for photons, \hat{a}^\dagger and \hat{a} respectively, the operator reads as follows:

$$\hat{H}_L = \hbar\omega_L \hat{a}^\dagger \hat{a}. \quad (\text{I.3})$$

The eigenstates of these two operators are ‘‘Fock states’’ and are represented by $|g, n\rangle$ and $|e, n\rangle$, where n is the number of photons in that state. Next, some well-known approximations for the laser field are applied that simplify the calculations enormously. First, for optical frequencies, the variation of the electromagnetic field of the laser on the order of the atom size can be neglected, and the atom can be approximated as a dipole. Then, the interaction term \hat{V}_{AL} is

$$\hat{V}_{AL} = -\hat{\mathbf{d}} \cdot \hat{\mathbf{E}}. \quad (\text{I.4})$$

Here $\hat{\mathbf{d}} = e\hat{\mathbf{r}}$ is the atomic dipole moment operator and $\hat{\mathbf{E}}$ is the electric field operator of the laser light.

The second approximation, known as the rotating wave approximation (RWA), assumes $|\omega_L - \omega_A| \ll \omega_L + \omega_A$ and neglects the fast oscillating term (see [2]). For a plane wave with an amplitude E_0 , the interaction term at a certain spatial position (choose $z = 0$) becomes

$$\hat{V}_{AL} = \frac{\hbar\Omega}{2}(\hat{a}e^{i\omega_L t}|e\rangle\langle g| + \hat{a}^\dagger e^{-i\omega_L t}|e\rangle\langle g|), \quad (\text{I.5})$$

where $\Omega := \frac{-eE_0}{\hbar} \langle e|r|g\rangle$ is the Rabi frequency. A transformation to a rotating frame gets rid of the phase factors and the Hamiltonian becomes, using $\Delta_L = \omega_L - \omega_A$,

$$\hat{H} = \hbar \begin{pmatrix} -\Delta_L & \frac{\Omega}{2} \\ \frac{\Omega}{2} & 0 \end{pmatrix}. \quad (\text{I.6})$$

The eigenvalues of this Hamiltonian are:

$$E_{e,g} = -\frac{\hbar\Delta_L}{2} \pm \frac{\hbar}{2}\sqrt{\Delta_L^2 + \Omega^2} \quad (\text{I.7})$$

In the limit of far detuning, $|\Delta_L| \gg \Omega$, the energy shift can be expanded to first order in Ω/Δ_L , yielding:

$$\Delta E_g = \frac{\hbar\Omega^2}{4\Delta_L} \quad (\text{I.8})$$

$$\Delta E_e = -\frac{\hbar\Omega^2}{4\Delta_L}. \quad (\text{I.9})$$

This is the Stark shift that induces the dipole moment, drawing the ground state atom into high intensities for red detuning ($\Delta_L < 0$) and repelling it from high intensities for blue detuning ($\Delta_L > 0$).

If an electrical field in the z direction is considered, the force acting on an atom is

$$F = - \left\langle \frac{\partial \hat{V}_{AL}}{\partial z} \right\rangle, \quad (\text{I.10})$$

since this is the relevant term of the Hamiltonian that describes the interaction. The result of this equation is [1]

$$F = \frac{\hbar s}{1+s} \left(-\Delta_L q_r + \frac{1}{2} \gamma q_i \right) \quad (\text{I.11})$$

where $s = I/[I_s(1 + (2\Delta_L/\gamma))]$ is the saturation parameter, $I_s = \pi \hbar c \gamma / (3\lambda^3)$ is the saturation intensity, γ is the decay rate of the spontaneous emission and $q_r + iq_i$ is the logarithmic derivative of the complex function Ω . It is defined as $\frac{d}{dz} \ln[\Omega(z)] = (q_r + iq_i)$. For a travelling electro-magnetic wave, $E = E_0(e^{i(kz-wt)} + cc.)$, the position dependence is only in the phase and therefore $q_r = 0$ and $q_i = k$. For a standing wave, $E = E_0 \cos(kz)(e^{-iwt} + cc.)$, $q_r = -k \tan(kz)$ and $q_i = 0$.

It can be seen that there are essentially two different forces acting on the atom. The first is the spontaneous scattering force, which acts in the direction of laser propagation

$$F_{\text{sp}} = \frac{\hbar k \gamma}{2I_s} \frac{I}{1 + I/I_s + (2\Delta_L/\gamma)^2}. \quad (\text{I.12})$$

It is related to the scattering rate Γ_{sc} in the following way:

$$F_{\text{sp}} = \hbar k \cdot \Gamma_{\text{sc}}. \quad (\text{I.13})$$

The other force is the optical dipole force, which acts in the direction of the laser

intensity gradient,

$$F_{\text{dip}} = \frac{2\hbar k \sin 2kz}{I_s} \frac{I \Delta_L}{1 + 4I/I_s \cos^2 kz + (2\Delta_L/\gamma)^2}. \quad (\text{I.14})$$

By taking a closer look at Eqs. (I.12) and (I.14), it can be seen why the laser for a dipole trap should be very powerful: The further the detuning Δ_L of the laser, the smaller the scattering rate, because it is proportional to I/Δ_L^2 . Since the dipole potential is just proportional to I/Δ_L , a deep dipole trap can still be achieved by using high laser intensities.

CHAPTER II

THEORY OF THE LASER

II.1. Interaction of Photons and Atoms

For the purpose of clarity and simplicity, we consider the most basic interaction between photons and atoms that make up a laser. Therefore, we restrict ourselves to a two-level system. For example, this could be an atom that has two states $|1\rangle$ and $|2\rangle$ corresponding to discrete energy levels E_1 and E_2 , respectively. All the other states are neglected. Furthermore, we consider only monochromatic light, so that all the interacting photons have the same frequency and therefore the same energy.

If the electromagnetic field of a light beam is coupled to this atom, three different types of interaction can take place.

A. Spontaneous Emission

If the system is initially in the upper state $|2\rangle$, the electron can drop spontaneously into the lower state $|1\rangle$. By doing that, the atom emits a photon of energy

$$E_{\text{ph}} = h\nu = \Delta E \tag{II.1}$$

where $\Delta E = E_2 - E_1$.

This emission is random in direction, phase, and time, with the result that the emitted light is incoherent.

The transition rate of this process is:

$$\left(\frac{dn_2}{dt}\right)_{\text{spont. em.}} = -\gamma n_2, \quad (\text{II.2})$$

where n_2 is the population density of the state $|2\rangle$, γ is the decay rate and the minus sign comes from the fact that n_2 is decreasing.

B. Absorption

Absorption occurs if a photon with resonance energy ΔE interacts with a system that is in the state $|1\rangle$. The energy of the photon is absorbed with a certain probability, and the system is raised into the upper state.

Since absorption depends on the light field as well as the population density n_1 of state $|1\rangle$, one can write the transition rate as:

$$\left(\frac{dn_1}{dt}\right)_{\text{stim. abs.}} = -B_{12}u(\nu)n_1, \quad (\text{II.3})$$

with

$$u(\nu) = \frac{8\pi h n^3 \nu^3}{c^3} \frac{1}{\exp(\frac{h\nu}{k_B T}) - 1} \quad (\text{II.4})$$

being the spectral energy density written in terms of Planck's black-body radiation formula of the stimulating photon field, B_{12} being the proportionality constant, and the minus sign again indicating the decreasing of n_1 .

C. Stimulated Emission

The final interaction is the inverse process of absorption. It is again an emission, but this time it is stimulated, meaning that the system is in the upper state when a photon with the resonance frequency interacts with it. The photon stimulates the system to drop into the lower state and emit another photon in the same mode as the interacting photon. This means that the emitted photon has exactly the same frequency, phase, direction of propagation, and polarization as the stimulating photon. This process can be used to amplify an optical beam because it is a coherent radiation. Light sources that produce light in this way are called LASERs (Light Amplification by Stimulated Emission of Radiation). Many atoms in state $|2\rangle$ are needed to get a reasonable amplification of the initial interacting light field. An ensemble of atoms having a greater population density in the upper state than the lower state is called “population inversion”.

Again, the transition rate depends on the spectral energy density $u(\nu)$ and the population density n_2 ,

$$\left(\frac{dn_2}{dt}\right)_{\text{stim. em.}} = -B_{21}u(\nu)n_2, \quad (\text{II.5})$$

with B_{21} being a proportionality constant.

II.2. Rate Equation

To describe the whole two-level system now, we must combine the three processes.

To this end, we follow the simple argument of Einstein who considered an ensemble of atoms in thermal equilibrium in the presence of a light field of spectral energy density $u(\nu)$.

Transitions from state $|2\rangle$ to state $|1\rangle$ comprise both spontaneous and stimulated emission, so the total transition rate r_{21} is

$$r_{21} = \gamma n_2 + B_{21}u(\nu)n_2 \quad (\text{II.6})$$

where γ and B_{21} are the Einstein coefficients of spontaneous and stimulated emission, respectively.

The transition rate from the lower to the upper state is only comprised of absorption,

$$r_{12} = B_{12}u(\nu)n_1 \quad (\text{II.7})$$

with B_{12} being the Einstein coefficient for stimulated absorption.

In thermal equilibrium both rates are equal, so that

$$\gamma n_2 + B_{21}u(\nu)n_2 = B_{12}u(\nu)n_1. \quad (\text{II.8})$$

Eq. (II.8) is known as the rate equation of a two level system. We will come back to this equation later, when we will discuss it in the context of the diode laser.

II.3. Elements of a Laser

The laser is essentially an optical oscillator. Parts of the output of this optical

resonator are fed back with the correct phase into the input. In order to achieve this, a laser usually consists of three elements.

The **active medium** is a medium with population inversion such that a light field propagating through it will be amplified by stimulated emission.

The **pump** delivers energy to the active medium so that there can be a population inversion. The pump can consist of a flash lamp, gas discharge or another laser. In the case of a diode laser, the pump is very convenient, as it is just an electrical current that places charge carriers in the active medium so that population inversion can be achieved.

Finally, an **optical resonator** is required. This is usually accomplished with a Fabry-Perot-Interferometer (FPI). Due to the boundary conditions of a FPI, only certain modes that form a standing wave inside the cavity can be excited. The condition for a standing wave is:

$$L = m \frac{\lambda_0}{2n_{\text{eff}}} \quad (\text{II.9})$$

with λ_0 being the vacuum wavelength, n_{eff} the effective refractive index of the cavity and $m = 1, 2, 3, \dots$.

The resonator stores some of the radiation emitted by the active medium in a few modes so that the number of photons in these modes is $n \gg 1$. This increases the probability of stimulated versus spontaneous emission. The resonator is also recycling

modes back into the active medium so that another cycle of stimulated emission is started by photons in the same mode and the laser light stays unaltered. The result is a light oscillator rather than a light amplifier.

For a semiconductor laser, the active layer also acts as the cavity. Using a coating on the front and back facets, the required reflectivity can be achieved. Depending on the index of refraction and the thickness of the layer, an antireflection coating can be applied. The standard material for this is Al_2O_3 , which also has the advantage of being able to passivate and protect the extremely sensitive facets. By alternating layers of Al_2O_3 and Si, a so-called Bragg reflector with a high reflection coefficient can be created. For high power diode lasers, the back facet is usually highly reflective, whereas the front facet is antireflection coated, so that the photon density inside the cavity is reduced. This effectively eliminates destructive interference from back reflection of the front facet and results in an increased output power.

II.4. The Principle of a Laser

Usually the active medium is surrounded by the resonator. One of the resonator's windows is partially transmitting so that the laser light can be extracted through it, but there is still enough reflection to maintain an oscillating wave in the resonator. Another crucial condition, of course, is that the pump provides enough power to compensate for the emitted laser beam and other losses.

If the active medium is in a state of population inversion, and the interacting

optical field is strong enough to make stimulated emission the dominant process, then an incoming photon of the right frequency will produce another photon emitted in exactly the same mode. Now, both of those photons can stimulate two other atoms to emit photons in the same mode, etc. This means that one incoming photon can produce an avalanche of photons in the same mode, and therefore the intensity of the electromagnetic wave traveling in the z-direction grows exponentially, neglecting gain saturation effects:

$$I(\nu, z) = I(\nu, 0)e^{\alpha(\nu)z}. \quad (\text{II.10})$$

When $\alpha(\nu) < 0$, this is known as Beer's law of absorption.

Since the resonator only sustains frequencies that correspond to wavelengths forming a standing wave in the resonator, only a few modes of the continuous gain spectrum are selected (Fig. II.1). Furthermore, only the modes where the resonator spectral line intersects the gain curve above threshold are amplified.

II.5. The Diode Laser

Semiconductors

Due to the overlap of the atomic orbitals in a semiconductor, the electrons aren't located in discrete levels as in a single atom. Instead they form a continuous "band structure." The band structure consists of a conduction and a valence band, separated by an energy gap E_g , which is typically 0.5 - 2.5 eV. The conduction band is filled with

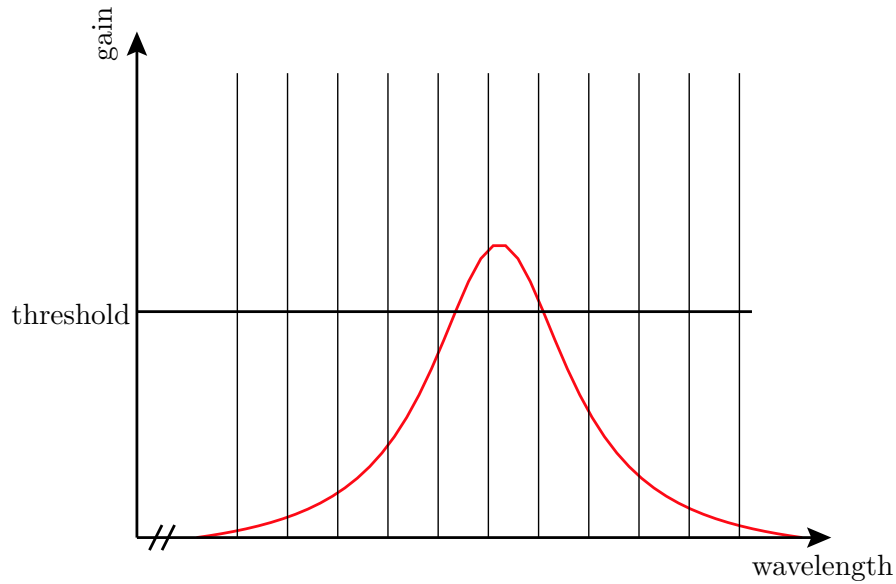


FIGURE II.1: Gain curve of a laser with the modes of the resonator.

electrons and in an undoped material there are as many holes in the valence band as electrons in the conduction band. Holes are “missing” electrons in the valence band that can also move and therefore conduct current. Due to the continuous band structure, the electrons in the conduction band and the holes in the valence band can move nearly freely and can thus be approximately described as an electron gas. Therefore, the electrons in thermal equilibrium in a semiconductor are Fermi-distributed,

$$f(E, T) = \frac{1}{\exp\left(\frac{E-E_F}{k_B T}\right) + 1}, \quad (\text{II.11})$$

where E_F is the Fermi energy. For $T = 0$ K, f becomes a step function with the value $f = 1$ for energies below the Fermi energy and $f = 0$ above E_F , which means that all electrons are in the valence band.

Doped Semiconductors

The properties of a semiconductor (where the atoms forming a semiconductor are in group IV) can easily be changed by doping it with atoms of groups III and V. If a semiconductor is doped with atoms of group V (P, AS,...), just 4 of the outer electrons of the atom take part in the chemical bonding, and one electron is very weakly bonded to the atom. The result is that the 5th electron has a very low ionization energy (≈ 0.1 eV or smaller). These electrons sit on an energy level that is higher than the energy of the conduction band and very close to the valence band. Therefore, the Fermi energy of the so-called n-doped semiconductor rises to this level.

For p-doping, one puts some atoms from group III (B, In,...), having just 3 outer electrons in the semiconductor, and instead of electrons with energies close to the conduction band, one gets holes with energies close to the valence band and a lower Fermi energy.

p-n Junction

If p- and n-doped semiconductors are brought into metallurgical contact, electrons and holes will diffuse from areas of high concentration to areas with low concentration due to thermal motion. Electrons go from the n to the p part, where they recombine with the abundant holes, leaving behind positively charged atoms. On the other hand, holes diffuse in the opposite direction and recombine with electrons leaving behind negatively charged atoms. Therefore, the area in the middle of the p-n junction, called the depletion layer, loses all its mobile charge carriers, and what remains are

just the fixed positive ions on the n side and the negative ions on the p side. As a result, an electric field (and therefore a potential) is built up between the two sides. In terms of the energy diagram, the p part has more negative charge, which raises the Fermi energy and vice versa for the n part. Since both parts are in contact, the Fermi levels align, producing a bend in the band structure (Fig. II.2).

If in addition an external potential is applied, the potential difference between the two layers can be changed. We will just discuss the forward-biased case, where a positive potential U is applied to the p side. In this case, electrons are sucked away from the p-doped part into the source causing the Fermi level (and therefore the band energy) to be lowered. The converse is true for the n-part, where electrons are injected. As a result, the potential barrier decreases, and it is easier for charge carriers to cross over.

The current depends on the voltage through the relationship [7]:

$$j = j_0(e^{eU/K_B T} - 1), \quad (\text{II.12})$$

where j_0 is the drift current.

This formula shows why this is also called a diode: for $U > 0$, we get an exponentially increasing current, that saturates for higher voltages.

Due to the external potential, the semiconductor is no longer in an equilibrium state. The Fermi energies of the valence and conduction bands, E_{F_c} and E_{F_v} , are becoming misaligned. As a result of this misalignment, there are two different Fermi levels in the depletion layer, which represent a state of equilibrium. To describe this

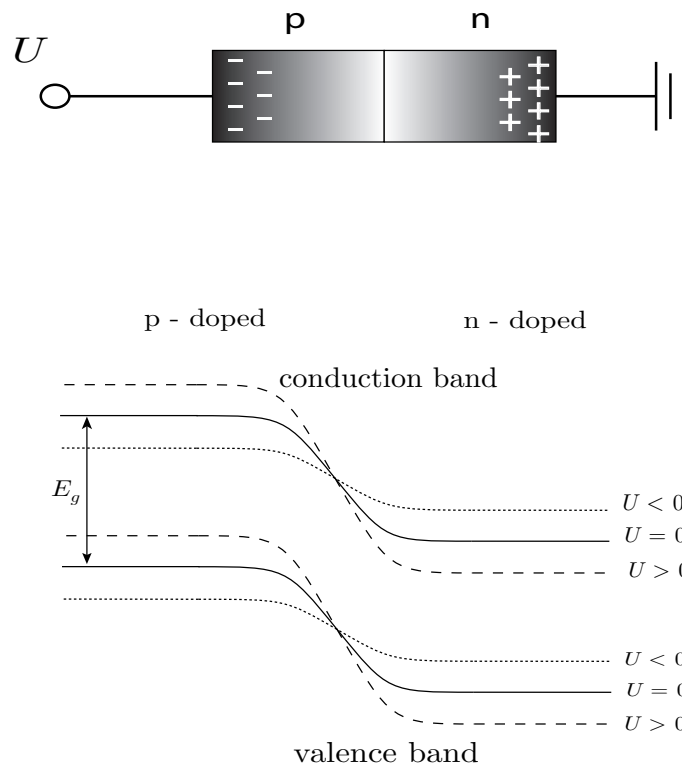


FIGURE II.2: p-n junction with an external potential U .

situation, two separate Fermi functions have to be considered. For the electrons in the conduction band and the holes in the valence band, we have, respectively,

$$f_c(E, T) = \frac{1}{\exp\left(\frac{E - E_{F_c}}{k_B T}\right) + 1} \quad (\text{II.13})$$

and

$$f_v(E, T) = \frac{1}{\exp\left(\frac{E - E_{F_v}}{k_B T}\right) + 1}. \quad (\text{II.14})$$

To confine the charge carriers to a small region of the diode, an additional layer is sandwiched between the p-n junction. This layer is not doped and has a smaller band gap than the other two layers. The energy diagram (Fig. II.3) shows that the electrons and holes of the injection current are directly transported to the area in the middle, where they remain confined by potential barriers on each side.

II.6. Absorption and Emission Revisited

With the knowledge of the two previous sections, a semiconductor interacting with light can now be described. As mentioned above, the ensemble of charge carriers in a semiconductor can be approximated as an electron gas. Therefore the energy takes the following form

$$E = \frac{p^2}{2m_0} = \frac{\hbar^2 k^2}{2m_{\text{eff}}} \quad (\text{II.15})$$

where m_{eff} is the effective mass. Using this effective mass, the charge carrier can be considered a free particle, but since it interacts with the rest of the atoms, it

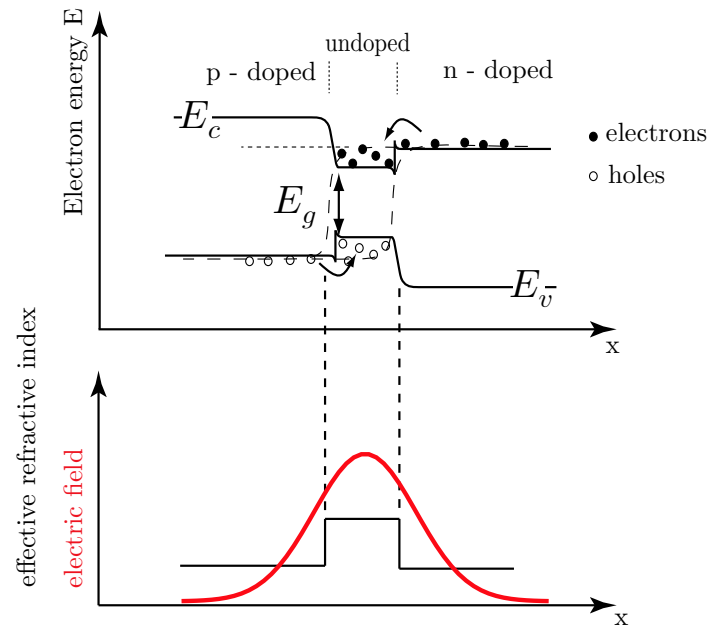


FIGURE II.3: Cut through a p-i-n heterostructure energy diagram, size of electrons and holes not to scale.

is actually located in a potential. Therefore, a mass depending on the potential is introduced.

For electrons, the energy has an offset of the band-gap E_g . Therefore the band structure takes the form of two parabolas. The parabola describing the holes is upside down, because holes have positive charge and the effective mass becomes negative. Since the momentum of photons is small compared to electrons, the emission of a photon doesn't change the momentum of the electron, and radiative transitions only occur at the same wave number k (Fig. II.4). Otherwise the transition would require another particle such as a phonon, which is unsuitable for lasers because of the low spatial phonon density. Since the particles tend to occupy the lowest energy

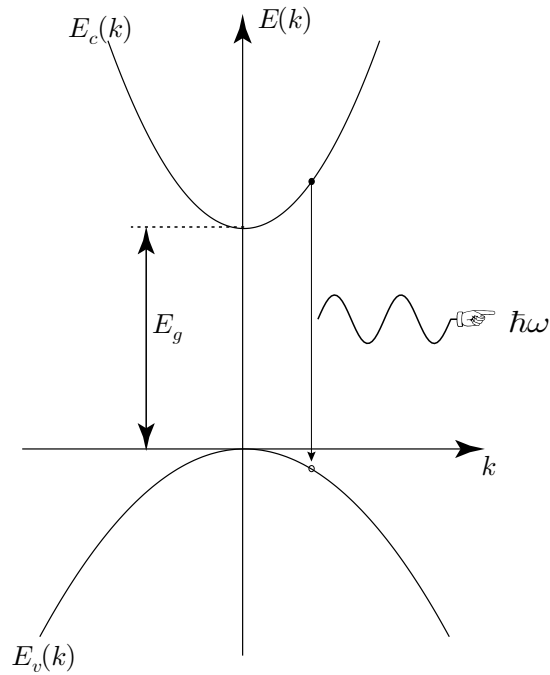


FIGURE II.4: One dimensional energy diagram for electrons and holes. E_c is the energy of the conduction band, E_v the energy of the valence band. An electron combines with a hole and a photon of energy $\hbar\omega$ is emitted.

states, it is necessary that the maximum and the minimum of the valence and the conduction bands have the same wavenumber k . Such a structure is known as a direct semiconductor.

Therefore, to describe the transitions of semiconductors for a fixed photon energy $\hbar\omega$, it is correct to consider the two-level system with discrete energy levels as mentioned above. However, in a semiconductor, the transition rate depends not only on the available charge carrier in one of the states but also on the missing charge carrier in the other band. Hence, the transition rate for spontaneous emission has to be

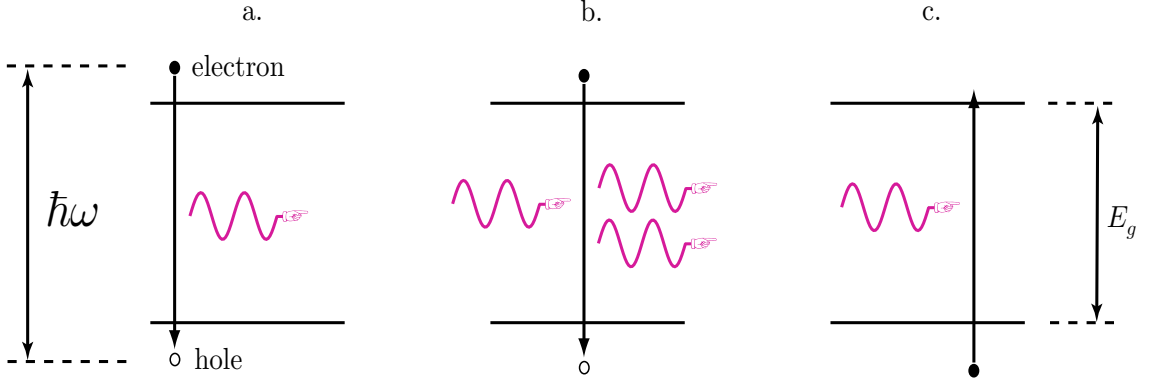


FIGURE II.5: Radiative transitions in semiconductors: a.) spontaneous emission, b.) stimulated emission and c.) stimulated absorption.

modified in the following way:

$$r_{\text{sp}} = AD(E_2)f(E_2, T)D(E_1)[1 - f(E_1, T)]. \quad (\text{II.16})$$

Here, $D(E_2)$ is the density of electronic states at energy E_2 and $f(E_2, T)$ is the distribution of the electrons, which is the probability that the states are occupied. The product $D(E_2) \cdot f(E_2, T)$ is therefore the electron density. Similarly, $D(E_1)$ is the density of electronic states at E_1 , and $[1 - f(E_1, T)]$ is the probability of a states not being occupied by an electron.

Since stimulated emission depends on the light field, the formula resembles Eq. (II.16) above, but using a different Einstein coefficient and incorporating the photon density $\rho(\hbar\omega) = u(\nu)/(\hbar\omega)$:

$$r_{21} = B_{21}\rho(\hbar\omega)D(E_2)f(E_2, T)D(E_1)[1 - f(E_1, T)]. \quad (\text{II.17})$$

Finally, in the process of stimulated absorption, a photon is absorbed and an electron-hole pair is produced. The rate depends on the electron density in the valence band

and the density of unoccupied states in the conduction band, as well as the light field:

$$r_{12} = B_{12}\rho(\hbar\omega)D(E_1)f(E_1, T)D(E_2)[1 - f(E_2, T)]. \quad (\text{II.18})$$

The ratio of the stimulated emission and absorption rates is essentially what determines whether a beam is absorbed or amplified. Using Eqs. (II.18), (II.17) with (II.13) and (II.14) gives the following relation, which does not depend on the density of states:

$$\frac{r_{12}}{r_{21}} = \frac{f_v(E_1, T)[1 - f_c(E_2, T)]}{f_c(E_2, T)[1 - f_v(E_1, T)]} = \exp\left[\frac{\hbar\omega - (E_{Fc} - E_{Fv})}{k_B T}\right]. \quad (\text{II.19})$$

Therefore, a crucial condition for the beam to be amplified is that $E_{Fc} - E_{Fv} > \hbar\omega$, in order to get a negative exponent.

Another instructive ratio is that of the spontaneous and stimulated emission rates:

$$\frac{r_{21}}{r_{\text{spont}}} = \frac{B}{A}\rho(\hbar\omega) = \frac{n^3}{\pi^2\hbar^3c^3}(\hbar\omega)^2\rho(\hbar\omega). \quad (\text{II.20})$$

Here, we see the importance of having a high photon density in order to get a good ratio of stimulated versus spontaneous emission. The optical waveguide and the Fabry-Perot resonator make it possible to achieve such high densities.

Finally, to get a power-current dependence, the rate equations for the electronic carrier density N_{carr} and the photon density N_{ph} are needed. The former is given by

$$\frac{dN_{\text{carr}}}{dt} = \frac{\eta_i j}{qd} - \frac{N}{\tau} - v_{\text{gr}}g(N, \lambda_0)N_{\text{ph}}, \quad (\text{II.21})$$

where the first term is the carrier generation rate, with η_i being the fraction of injected current that enters the active region, j the current density, q the elementary charge,

and d the thickness of the active region. The second term describes the rate of carriers that recombine without contributing to the laser beam (i.e., those which are non radiative, mainly the Auger recombination and the recombination at point defects), and recombination resulting in radiation of spontaneous emission. The last term is the rate of carriers that recombine in a stimulated emission process, with v_{gr} being the group velocity in the medium and $g(N, \lambda_0)$ the material gain.

For the photon density in the cavity we have

$$\frac{dN_{\text{ph}}}{dt} = v_{\text{gr}}\Gamma g(N, \lambda_0)N_{\text{ph}} + \Gamma\beta_{\text{sp}}r_{\text{sp}} - \frac{N_{\text{ph}}}{\tau_{\text{ph}}}, \quad (\text{II.22})$$

where the first term is the stimulated emission term multiplied by the confinement factor Γ , which takes into account the fact that the volume for the photons is larger than the volume for the carriers (the rates are normalized per unit volume). The second term is the rate of spontaneous emission with β_{sp} being the fraction that are emitted into the lasing mode. The last term describes the photon losses where τ_{ph} is the photon lifetime in the laser.

A good approximation for high power lasers is to neglect spontaneous emission ($\beta_{\text{sp}} = 0$). The steady state ($dN_{\text{carr}}/dt = dN_{\text{ph}}/dt = 0$) solution therefore yields two results. The first,

$$N_{\text{ph}} = 0, \quad (\text{II.23})$$

describes the laser below threshold. The other solution describes the device operating

above threshold,

$$N_{\text{ph}} = \eta_i \frac{1}{qdv_{\text{gr}}g_{\text{th}}}(j - j_{\text{th}}), \quad (\text{II.24})$$

where g_{th} is the constant gain above threshold, and j_{th} is the threshold condition for the current. Eq. (II.24) can be used to calculate the optical power of the beam by noting that the energy stored in a Fabry Perot resonator is

$$E_{\text{FP}} = N_{\text{ph}}\hbar\omega V_{\text{ph}}, \quad (\text{II.25})$$

where V_{ph} is the volume occupied by photons. The last term of Eq. (II.22) represents the loss of the photons and can be separated into two parts: the intrinsic loss α_i and the output of the laser beam through the window α_{mirror} . Therefore, the photon density of the output through the mirror is

$$\frac{dN_{\text{ph}}}{dt} = -\alpha_{\text{mirror}}v_{\text{gr}}N_{\text{ph}}. \quad (\text{II.26})$$

Finally the power of the output beam, using Eqs. (II.25), (II.26) and $I = jV$ is given by

$$P = \frac{dE}{dt} = \eta_i \frac{\alpha_{\text{mirror}}}{\Gamma g_{\text{th}}} \frac{\hbar\omega}{q}(I - I_{\text{th}}) \quad (\text{II.27})$$

From this equation, it can be seen, that above threshold, the power of the laser light increases linearly with the current.

The p-i-n Heterostructure as a Diode Laser

With the p-i-n heterostructure (Fig. II.3), many things can be accomplished. First of all, as mentioned above, the undoped layer defines a small area where recombination

processes can happen. In this region, the condition for amplification of laser light (II.19) is also fulfilled.

Furthermore, the p-i-n structure acts as a waveguide using total internal reflection, because the undoped layer has a higher refractive index than the cladding layers around it. Since the thickness of the layer is small enough, only the fundamental mode with a nearly Gaussian field distribution is able to propagate through it. This is known as an index-guide.

To further improve the structure, quantum wells are embedded in the undoped area (Fig. II.6). Quantum wells are square potentials of the size of 5-10 nm. At this size, the electronic wave functions show quantization effects in the vertical direction. Because of the smaller active volume and the quantization effects, higher carrier densities in a narrower energetic distribution can be achieved. This has the advantages of a lower threshold, higher gain and smaller spectral shift due to band-filling effects. However, the most important advantage of a quantum well structure is that the wavelength can be changed. By incorporating a certain type of atom, a tensile strain can be introduced because of the atomic lattice mismatch between the changed and the unchanged areas.

II.7. TE & TM Polarization

The emitted light of diode lasers is linearly polarized, but may have different polarization directions: TE (transverse electric) which is perpendicular to the propagation

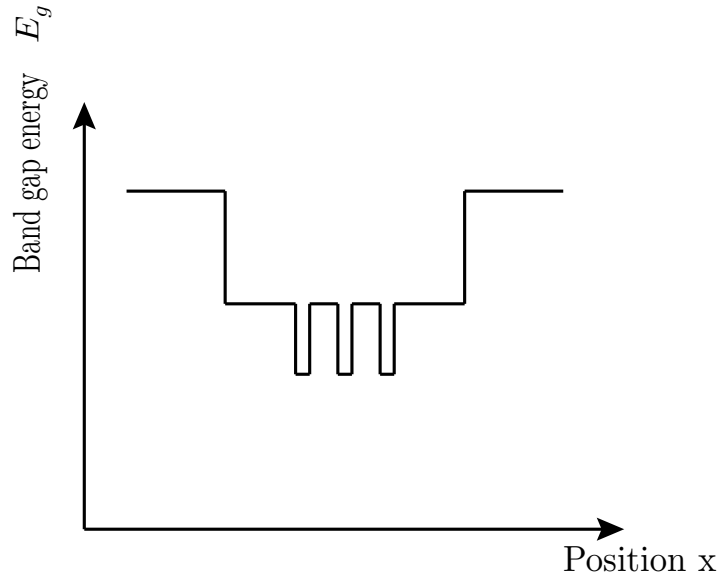


FIGURE II.6: Energy diagram of a multi-quantum well surrounded by a confinement structure.

direction and perpendicular to the growth direction of the semiconductor, and TM (transverse magnetic) which is parallel to the growth direction.

To describe the polarization of a diode laser, we must consider a more detailed model of the band structure, in which the valence band consists of three sub-bands. The sub-bands are a result of the 4p state of the GaAs “molecule” in which the spin-orbit coupling leads to the total angular momentum $j = 3/2$ and $j = 1/2$. Here, we only consider the $j = 3/2$ states and refer to $m_j = 3/2$ and $m_j = 1/2$ as “heavy holes” and “light holes”, respectively.

These two sub-bands are usually degenerate at the momentum state $\mathbf{k} = \mathbf{0}$. But for example in a strained quantum well device, as described above, the bands can split up.

To find the probability for a radiative transition, the dipole moment matrix element is calculated by

$$\mu_{if} = \langle i | \hat{\mathbf{d}} | f \rangle, \quad (\text{II.28})$$

where $|i\rangle$ is the initial (electron) state, $|f\rangle$ is the final (hole) state and $\hat{\mathbf{d}}$ is the dipole operator from Eq. (I.4). This becomes $\langle i | ez | f \rangle$ for TM polarization and $\langle i | ex | f \rangle$ for TE polarization.

Plugging in the correct wave-functions and using the symmetry dependence of the electronic, the heavy and the light hole states, we find that the TM dipole matrix element only couples the electron to the light hole state [9]. Whereas the TE dipole matrix element couples the electron to both the heavy and light hole states, depending on the carrier momentum. However, for $k \approx 0$ it couples mostly to the light holes.

So, the radiation may have a different polarization, depending on the strain of the quantum well and therefore on the lasing frequency.

II.8. Current, Temperature and Frequency Dependence

The wavelength of the emitted laser light of a diode depends primarily on the energy of the band gap E_g , but by manipulating the injection current and the temperature of the diode, it can be changed within a bandwidth of up to 30 nm [19].

The wavelength of the light responds to temperature changes because the optical path length of the cavity, the refractive index and the gain curve are temperature dependent. However, the sensitivity to each of these effects is quite different. For

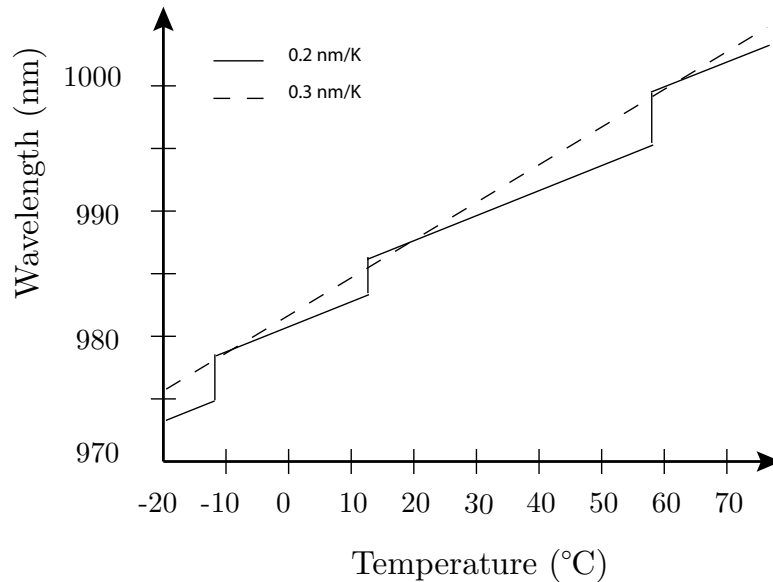


FIGURE II.7: The peak emission wavelength of a diode laser. The dashed line represents the change of the peak gain and the solid line the changes of the cavity length and the refractive index. After [3].

an AlGaAs diode, the optical length of the cavity and the refractive index have a combined effect on the wavelength of about 0.06-0.2 nm/K. The gain curve changes by about +0.33 nm/K, due to the variation of the gap between the energy bands. This makes the overall temperature-wavelength curve appear as a sloped staircase (Fig. II.7). The discrete steps in the staircase are due to hops between different modes of the resonator. The slope of the individual stairs originates from the continuously changing cavity length, which changes the resonance frequency.

Changing the injection current has two effects on the laser diode. First, it changes the temperature and second, it changes the carrier density in the active zone, which in turn changes the refractive index. Since a higher current produces Joule heating, this effect looks very much the same as the temperature-wavelength dependence. The

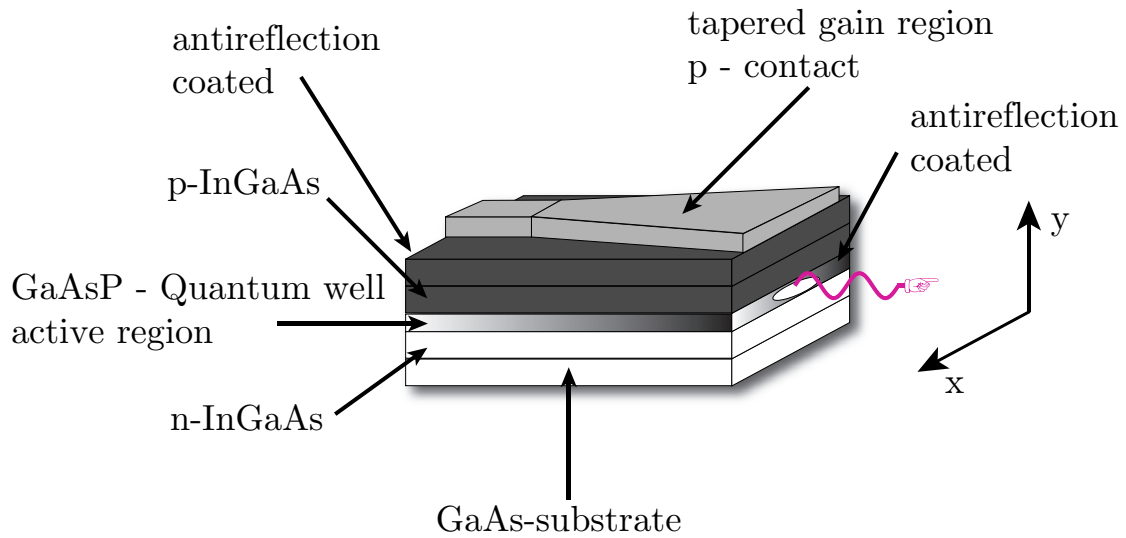


FIGURE II.8: Schematic drawing of a tapered amplifier.

change of the refractive index is small and only matters for high-frequency modulation of the current.

II.9. The Tapered Amplifier

In order to maintain a single spatial mode, the transverse dimensions of the waveguide of a conventional semiconductor laser have to be on the order of the wavelength. This confinement limits the output power of the laser due to heating of the bulk and the facets. On the other hand, devices with a much broader gain region, like broad area lasers, can produce higher intensity light, but they oscillate in very high order lateral modes. The tapered amplifier combines these two essential features. As depicted in Fig. (V.1), it consists of two parts: a straight index-guided waveguide section and a gain-guided tapered section. The beam of the master oscillator is

coupled into the small end and then expands laterally because of diffraction, filling the tapered gain region of the device. The straight part is used as a modal filter to excite only the fundamental transverse mode and it has the advantage that only a low input power is needed to achieve sufficiently large energy densities. By just using a small-sized straight guide, the laser could not reach such high powers. Those high power densities would give rise to the nonlinear optical Kerr effect which would change the refractive index depending on the light intensity. This would lead to a self-focusing effect and destroy the material. The tapered section therefore makes sure that the energy density is kept below the critical value, while still achieving high output powers that maintain the single mode behavior. However, the beam shape is still altered through undesired power-dependent changes of the charge carriers and temperature induced refractive-index perturbations that decrease the beam quality and brightness. A typical length of the tapered region is about 2-3 mm and the input aperture of 5-10 μm expands to about 200 μm . Electrical contact is established by metallizing the top and bottom layers. The front and back facets are anti reflection coated ($R_f \approx 0.1\%$) to assure a low energy density in the cavity, a suppression the laser's eigenmodes and minimal reflection. Such reflection can lead to destructive interference and irregular intensity fluctuations, which in turn can result in multi-mode behavior.

To understand the tapered amplifier, a simple and descriptive model is presented. The input beam is focused tightly enough into the input aperture, so that after the

waveguide, it diffracts with the angle of the taper and fills out the whole gain medium. If the gain medium is long enough, the spontaneous emission is small compared to the stimulated emission, initiated by the input beam. Since the gain region is pumped by a spatially homogeneous current density, the gain along the propagation axis is uniform. But since the gain varies with the inverse of the local optical power density, it is not laterally uniform. This means that an incoming Gaussian beam experiences a lower gain at the center than in the outer regions because it saturates first for larger intensities. As a result, it approaches a more and more flat-hat distribution, which is uniform over a certain area and zero outside. Due to perturbations from this model such as carrier diffusion, non linear and thermal effects and non uniform carrier injection, the intensity pattern will deviate from this model, but nevertheless, a good understanding of the amplifier can be extracted from it.

Since the beam expands from the small waveguide and diffracts at the tapered angle, the amplitude and phase will be uniform along the curved wavefronts extending from the aperture, but not along the flat surface of the emitting facet. However, a uniform phase along the surface (and therefore a diffraction-limited beam) can be obtained to a high degree of approximation. After the beam is emitted from the front facet, it obeys Snell's law. For small angles, the diffraction angle is the angle of the taper times the lateral modal index n_l . For a taper angle of $\approx 6^\circ$ this yields a diffraction angle of about 20° . Since the wavefronts are not perfectly planar but curved, the beam emitted by the wide aperture seems to emanate from a point inside

the diode. This virtual source point is a distance of approximately L/n_l behind the output facet, where L is the length of the amplifier. On the other hand, the beam profile perpendicular to the wide side of the facet is diffracted at the facet with an angle of 30-40°. Thus, it can be seen that the beam is astigmatic, which means that it has different focal points for the two perpendicular directions after it propagates through a spherical lens.

To get the far-field distribution in the horizontal plane, an ideal cylindrical lens is placed a focal length f away from the aperture. Therefore, the Fresnel integral for the propagated field has to be solved:

$$E(x, y, z) \propto \iint_{-\infty}^{+\infty} E_0(x', y') e^{-i\Phi(x', y')} e^{\frac{-ik_0}{2z}(x'^2 + y'^2)} e^{i(k_x x' + k_y y')} dx' dy'. \quad (\text{II.29})$$

here, $k_0 = \omega_0/c$ is the wavenumber, ω_0 is the frequency of the light, $E_0(x', y')$ is the electrical field at the aperture, $\Phi(x', y')$ is the phase induced by the cylindrical lens and $k_x = \frac{k_0 x}{f}$. The second term in the integral, the induced phase by the lens, is chosen such that the product with the quadratic phase-curvature term, the third term in the integral, is equal to unity. This means that the far-field intensity pattern is the squared Fourier-transform of the field distribution at the output facet.

To calculate the far-field of the TA, the flat-hat distribution with a uniform phase at the output facet is considered. Considering that the thin lens, by definition, just affects the phase of the beam, one can calculate the the lateral power density as a function of angle $P(\phi)$. This is nothing other than the squared Fourier transform of

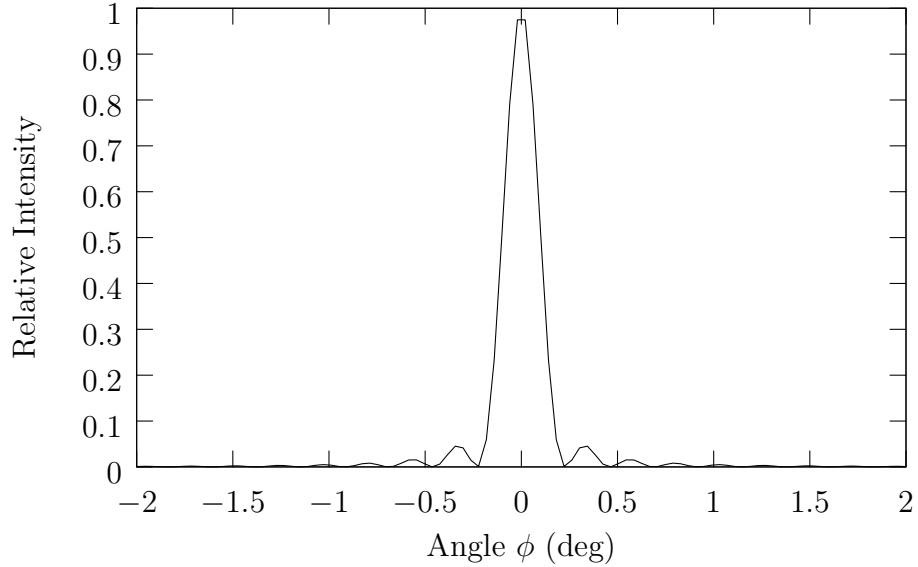


FIGURE II.9: Far-field intensity pattern of a tapered amplifier.

the flat-hat distribution [5]

$$P(\phi) \propto \frac{\sin^2[D\pi \sin(\phi)/\lambda]}{(\pi D \sin(\phi)/\lambda)^2}, \quad (\text{II.30})$$

with D being the width of the output facet, ϕ the far-field angle and λ the emitted wavelength. From Eq. (II.30), we can see that approximately 90% of the beam intensity lies inside the central lobe of the far field pattern (Fig. II.9.)

The field at the output facet is in reality not flat-hat distributed. Deviations from the ideal distribution lead to far-field patterns where the size of the central lobe doesn't change much, but the fraction of energy inside the lobe does. Therefore, an analysis of the near-field can show degradations of the amplifier. Some reasons for degradations are [5]: non-uniformities in the electrical and optical properties of the

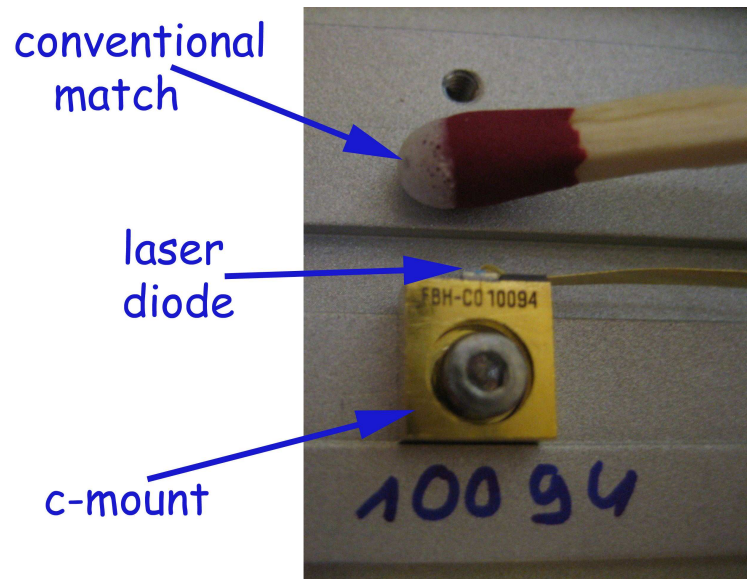


FIGURE II.10: Picture of the tapered amplifier compared to a match. The golden colored part is the c-mount of the diode. The real diode is the small blue dot on top of the mount. It appears to be blue in this picture but it is black in reality.

material, strains introduced by fabrication and packaging and heat sinking, strains at the edges of the tapered region where the metal layers are deposited, non-linear self-focusing effects, spatial hole burning effects and spatial fluctuations in the seeding beam.

The amplifier diode is mounted upside down on a c-mount (Fig. II.10), which acts as a heat sink and an electrical contact. The n-side is contacted by wire bonding.

CHAPTER III

THE EXPERIMENTAL SETUP

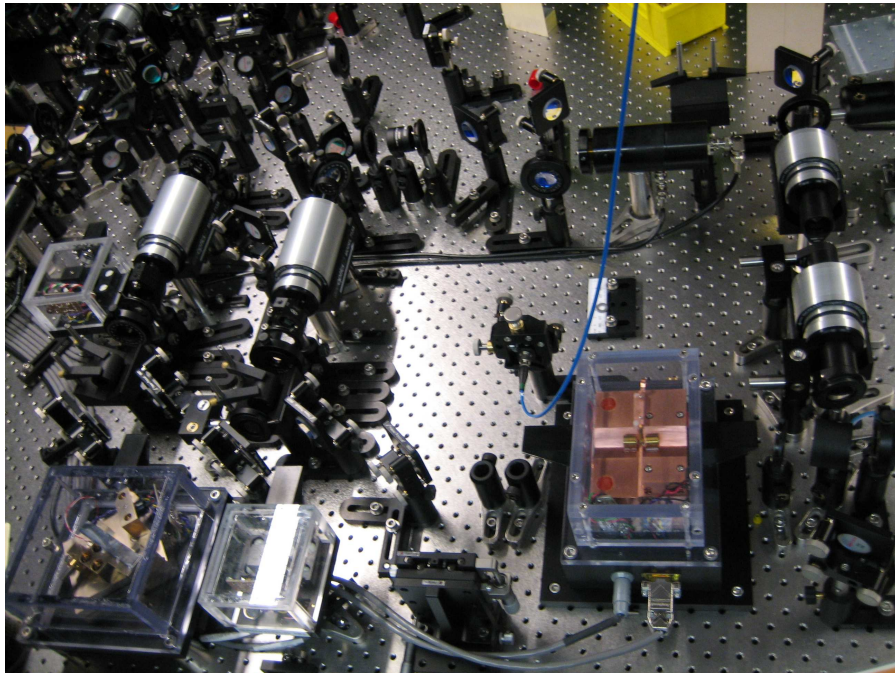


FIGURE III.1: Picture of the optical setup.

III.1. The “Lasers” s

The optical setup consists of three lasers. The master laser is injection-locked to the slave laser, which in turn is coupled into the tapered amplifier.

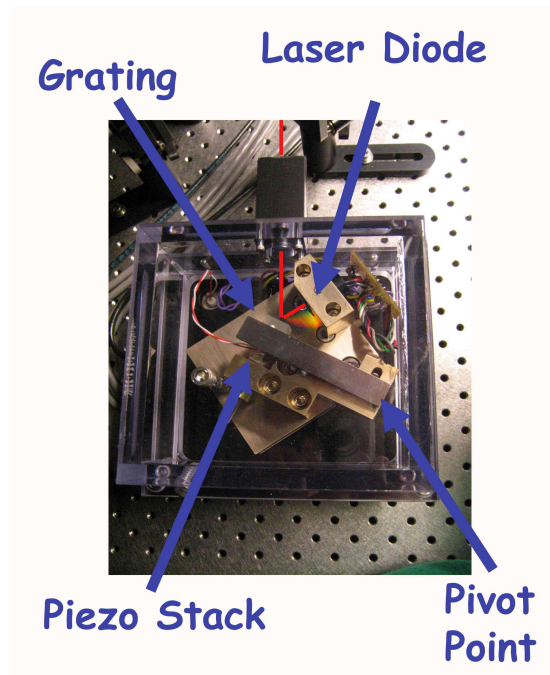


FIGURE III.2: Picture of the master laser. The path of the laser beam is indicated by the red line.

III.2. Pseudo-External-Cavity Laser or the “Master”

A common way to achieve a narrow linewidth single mode operation with diode lasers is to use the reflection of an external grating as an extended cavity. The master laser is built in a Littrow configuration, which means that the beam of a laser diode with a low-reflectance front facet is collimated with a lens and then reflected by a grating. The zeroth order of the reflection is coupled out as a single-mode beam, and the first order is coupled back into the diode. Therefore, the frequency of the reflected light depends strongly on the angle of the grating. Since the reflection of the grating is stronger than the reflection of the front facet, the grating provides

frequency-selective feedback and acts as one of the mirrors of the extended cavity. The other mirror is the back facet of the diode. The frequency of the laser can be tuned by changing the current and the angle of the grating via a piezo stack. The output beam has a linewidth < 5 MHz. In order to achieve a mode-hop-free operation, the angle, the current and the temperature need to be adjusted. However, because of the competition between the free-running modes of the diode and the extended-cavity modes, the tuning range is not truly mode-hop free, yet scanning over the rubidium spectrum is possible without mode hops. However, by locking the laser frequency to an atomic absorption line, long-term stability can be obtained.

Single-mode lasing properties are highly preferable, since other modes also draw power in multi-mode lasing operation, which results in higher overall power consumption and less power in the desired mode. Furthermore, multi-mode operation has more noise due to the competition between the different modes.

The master laser used in the lab is design from Mark Raizen's group at the University of Texas, modified for 780 nm. It uses a commercially available laser diode from Sharp (GH0781JA2C), with an output of 120 mW at 140 mA. The front facet of this diode is not anti reflection coated, which makes the laser a pseudo-external-cavity laser. The frequency is locked via a lock-in amplifier to a cross over line of the saturated-absorption rubidium spectrum. The frequency of the diode can be modulated and swept by applying a voltage to the piezo and changing the current. See [16] for more detailed information.

III.3. Frequency Stabilizing the Master Laser

The master laser is passively frequency stabilized. This laser and another already stabilized laser are coupled into a comparing cavity that is able to scan the frequency range by moving one of the mirrors. By measuring the slope of the transmission curve $dI_T/d\lambda$, it can be seen whether or not the lasers are locked.

The reference laser is locked to a cross over of the rubidium spectrum. To get a very precise lock, the beam is coupled into a Doppler-free absorption setup. Here, the laser is splitted into a strong pump and a weaker probe beam. Both beams propagate through a rubidium vapor cell, but in opposite directions at slightly different angles. Since the velocities of the rubidium atoms in the cell are Maxwell-Boltzmann distributed, the cell shows a Doppler-broadened absorption spectrum. Now, if the frequency of the laser coincides with a transition frequency of the rubidium, the pump laser excites atoms and their population is transferred to the upper state. Therefore, the probe beam doesn't get absorbed and if the frequency of the laser is scanned, the "Lamb dip" can be seen in the absorption spectrum. This only happens at atomic resonances because for other frequencies, the pump and the probe beam excite different Doppler-shifted atoms moving in opposite directions. For example, the laser frequency is above the resonance frequency $\omega_l = \omega_0(1 + \frac{v_z}{c})$ and the probe beam is propagating in the direction of the positive z -axis. The pump beam is in resonance with atoms moving towards it (i.e., atoms moving in the positive z -direction with v_z).

On the other hand, the probe beam is in resonance with atoms moving in its direction with $-v_z$. That means that the pump beam excites atoms of a different velocity class than the probe beam and therefore, the probe beam gets absorbed. Ergo, no dip can be seen in the absorption curve.

The cross transition, mentioned above, can happen if two atomic transitions, ω_1 and ω_2 ($\omega_1 < \omega_2$), overlap within their Doppler width and have the same common upper or lower level. If the laser frequency is tuned to $(\omega_1 + \omega_2)/2$, the pump beam excites the ω_1 transition of atoms moving toward the beam with the appropriate velocity and the ω_2 transition of atoms moving away with the appropriate velocity. Since the probe beam also excites these transitions, it cannot be absorbed. In other words, it would excite the ω_1 transitions of atoms moving toward the beam, but the probe beam has already excited the ω_2 transition of these atoms (moving away from the probe), and vice versa for the ω_2 transition. Therefore, in addition to the Lamb dips at ω_1 and ω_2 (for $v_z=0$), another dip in the absorption spectrum can be observed, the so-called cross-over dip in the middle of these frequencies. Usually, the cross-over dips are stronger than the normal dips and therefore more suitable to lock the laser. It is better to lock the laser to the center of the peak. To get a higher feedback, it is locked to the zero crossing of the derivative. The error signal is fed back to the grating and the injection current.

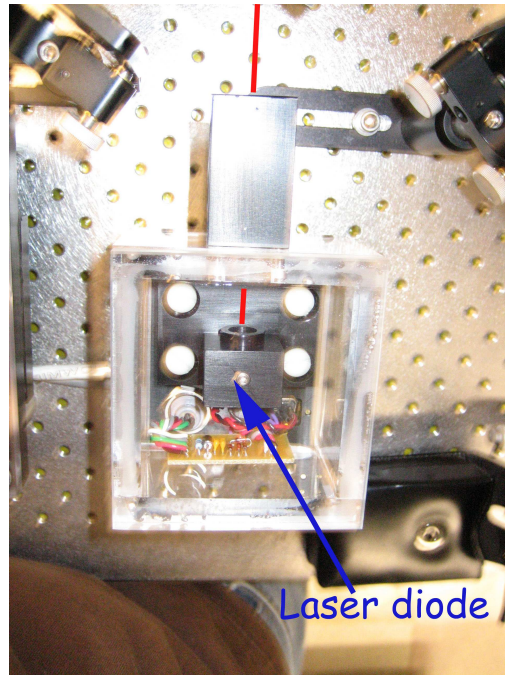


FIGURE III.3: Picture of the Slave Laser.

III.4. Slave Laser

The master-slave setup was chosen to ensure that the master laser alone does not have enough power to saturate the amplifier. After an amplifier diode died with no apparent reason, personal contact with Sacher Laser revealed that the power of the seeding laser was chosen too high and the diode possibly died because of this reason. The setup is kept, but the power of the slave laser is attenuated. Another reason could be outlet surges since shortly after that two other laser diodes (from two master lasers) died and a fuse of a laser current-driver blew.

In a master-slave setup, the master laser is injection-locked to a free running laser

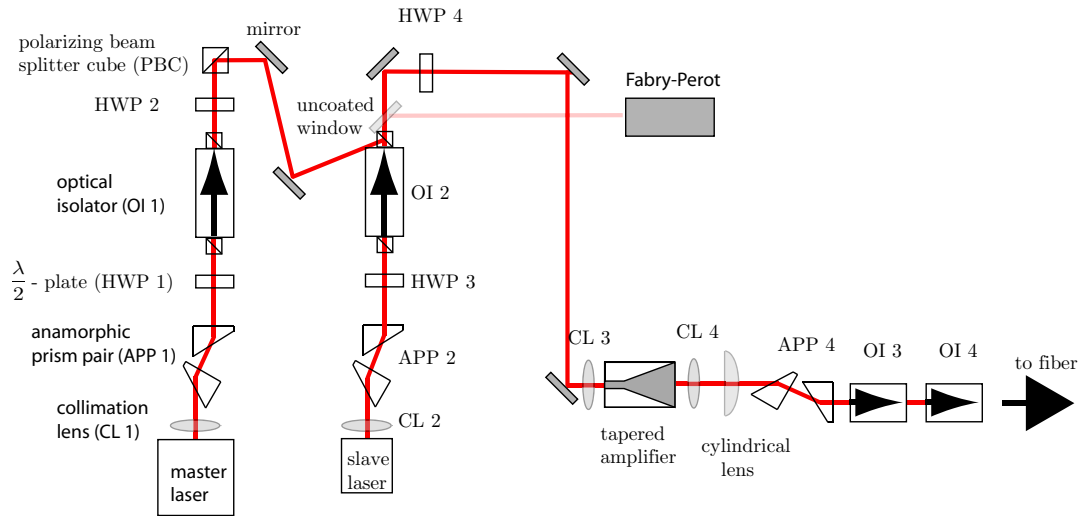


FIGURE III.4: Schematic of the optical setup.

in order to get the same (single) mode laser beam as the master, but with a higher output power. The diode of the slave laser is the same as that of the master laser. It is mounted in a simple temperature-stabilized housing. The output power of the slave laser is 100 mW with the same narrow linewidth of < 5 MHz as the master laser.

III.5. Optical Setup I

After collimating the master laser beam, it shows an elliptical profile, therefore it is circularly shaped using a 2:1 anamorphic prism pair. These are a pair of prisms positioned such that the beam propagating through them changes in one dimension. The relative angles of the two prisms change the unidirectional magnification. An

optical isolator (OI 1, Conoptics 713A) with 40 dB isolation protects the laser from back reflections. This is necessary because diode lasers are very sensitive to back-reflected light. The appropriate polarization for the OI is achieved by using a half wave plate. To control the power of the master laser beam, it propagates through another half-wave plate and reflected from a polarizing beam-splitter cube. After that, the beam is coupled into the optical isolator that protects the slave laser (OI 2, also Conoptics 713A). The beam of the slave laser propagates through an identical setup. After the beam exits through the output port of OI 2, the polarization is rotated again to inject it into the tapered amplifier. As mentioned above, diode lasers are very sensitive to the direction of the polarization.

III.6. Injection Locking the Master to the Slave Laser

Since the spectral gain of a diode laser is broad, a free running diode laser can be described as a spectrally white source. The frequency of the spontaneous emission is filtered by the Fabry-Perot resonator and above threshold the spectral linewidth of the laser is related to the width of the resonator modes.

By contrast, an injection-locked diode works differently. A beam of high spectral purity is coupled into the free running diode. Therefore, the initial photon source that starts the avalanche effect originates from the broad spontaneous emission as well as from the spectrally sharp injected beam. The stimulated emission is initiated by the injected light and the charge carriers in this energy state are depleted. Thus,

the gain at that frequency initially decreases, but recovers due to carrier scattering inside the energy band. These carriers can't contribute to the amplification of the other modes and they "lose" the competition against the frequency of the injected beam. Therefore, the slave adopts the spectral purity of the master laser and the output is a powerful beam with a narrow spectral resolution.

In order to injection lock the slave to the master laser, the beams of the two lasers must spatially overlap so that the modes of both lasers can be matched. This is done by coupling the beam of the master laser into the optical isolator of the slave laser (OI 2) using the appropriate polarization. Since the optical isolator has Glan polarizers as polarization splitters, the angle of the rejected beam is not 90° , but about 23° smaller. To check if the lasers are injection locked, the beam of the slave laser is coupled into a Doppler-free saturated absorption setup. If the hyperfine transitions of the rubidium vapor are observed, single-mode operation can be verified. Another part of the beam is reflected into a Fabry-Perot cavity. The length of the cavity can be changed by a piezo element and therefore, by ramping a voltage across the piezo, a small frequency bandwidth can be scanned.

To get the slave laser diode close to the right frequency, the current and temperature have to be adjusted. This is observed by fluorescence in a vapor cell. The slave laser can only adopt the behavior of the master if it operates in the vicinity of the correct frequency. In order to lock it, the current of the slave laser had to be slightly adjusted after injecting the master laser. After the optical isolator is set up

for the slave laser, the injection of the master laser is done by using two mirrors. A coarse alignment was achieved by rotating the input window of the optical isolator, such that a small amount of the slave laser beam is coupled out through the rejection window. The beams of the master and the slave laser can now be overlapped. If this is done well enough, the slave laser should follow the frequency of the master laser. After turning the isolator window back in the correct position, the frequency of the master is swept. If the hyperfine structure is observed, single-mode behavior can be verified. It is useful to have a look at the signal of the ramped Fabry-Perot cavity on the oscilloscope. If the beams are not locked, the high intensity steady modes of the slave laser and a small moving peak from the master laser should be observed. By stopping the frequency sweep of master laser, two different peaks can be observed on the oscilloscope. Changing the current of the slave laser changes the intensity of the two peaks. More precisely, one peak becomes bigger and the other one smaller. This procedure can be continued until locking is achieved. If the lasers are locked, the two peaks of the different lasers collapse to one high intensity peak. To make sure that this is the locked peak and not simply the slave laser peak, the frequency of the master can be swept again to verify that the peak moves with the sweeping frequency of the master.

To fine-tune the injection, the power of the master laser is lowered using a half-wave plate and a polarizing beam-splitting cube for as long as the locked signal of the FPI can be observed. If the laser becomes unlocked, the mirrors are readjusted until

the locked signal is observed again. This process is iteratively done until a low input power (in our case 1.2 mW) is achieved. Once the laser is locked, the current of the master or the slave laser can be changed over a wider range, or the input power can be lowered while the slave laser remains locked. If the changes are too big and the system loses lock and the easiest way is to go back to values that are known to lock the slave laser.

III.7. Injecting the Slave Laser in the Tapered Amplifier

A standard procedure [4] was used to couple the beam of the slave laser into the TA. First, the amplified spontaneous emission (ASE) of the free running amplifier is collimated at the front and back facets. Two mirrors are used to spatially overlap the ASE of the amplifier and the beam of the slave laser, so that it can be coupled into the input facet of the amplifier. The collimation lenses are glued to a three dimensional translation stage. After the correct position is found, they are glued to glass rods to hold them stably in position. Now, single-mode amplified light from the slave laser should be observed. For the fine tuning, the output power of the amplifier is observed and maximized by moving the lens and the mirrors. The intensity depends strongly on the position of the lens and especially on the distance to the diode. The lens was glued to a post, which was rigidly mounted at a 90° angle and attached to another post, which was in turn mounted on the translation stage. Even slight disturbances such as blowing against the translation stage and leaning on the optical table changed

the output due to the long lever arm of the translation stages.

The input power of the driving laser should be chosen very carefully. If it is too high, the amplifier can degrade very fast, because the transition between the waveguide and the tapered structure can be damaged. Since this part is located in the middle of the diode, nothing can be observed from the outside. Therefore, the diode should be operated with just the minimum seed intensity to saturate it. To measure that intensity, a standard procedure is to run the tapered amplifier at 2000 mA, increasing the power of the master laser to the point where the amplified light doesn't show a linear slope anymore. With very good mode-matching, this power should be anywhere from 5-7 mW and up to about 20 mW.

III.8. Optical Setup II

The output of the TA is collimated using the same lens as the input collimation lens. However, the beam shows a high degree of astigmatism, which means, that it has different focal lengths for the horizontal and the vertical directions. To correct for this, a cylindrical lens is used. As shown in Fig. III.5, the cylindrical lens just affects the beam parallel to the wide output facet. Back-reflections should be prevented in any circumstances, because they can destroy the diode. Therefore, all optical elements are slightly tilted. Two optical isolators (Conoptics 712 B) are used to prevent the diode from any back-reflection in the later setup. These isolators were chosen because they have a total isolation of 80 dB and are cheaper than the single unit with 60 dB

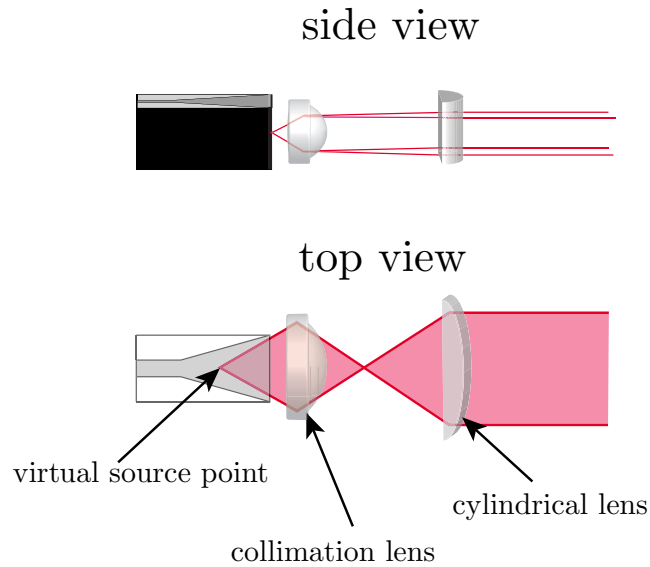


FIGURE III.5: Tapered amplifier with the out-coupling optics to compensate for the astigmatism.

isolation. About 85% of the total intensity is transmitted. After that, the beam is reshaped by a 3:1 anamorphic prism to couple it into a single-mode optical fiber. For a dipole trap, a high beam quality is necessary. The single-mode fiber acts as a spatial and a spectral filter to purify the beam. The transmission for the ASE background through the fiber is not very good, since it is spatially displaced from the center lobe. Since the frequency of the dipole trap is detuned and any frequency residue of the atomic resonance frequency is harmful for the trap, a vapor cell is placed before the fiber to absorb all resonant frequency components.

III.9. Handling of the Tapered Amplifier

Since the amplifier comes in an open heatsink package, there is no protection for the laser chip. The bare facets are especially delicate. Therefore, one should be careful in handling the tapered amplifier. The following section discusses some of the most critical causes for the death of a diode, besides from obvious reasons such as failing to operate it within the specifications.

The exposed laser facets must not be contaminated with any foreign material since contaminations can cause immediate and permanent damage to the laser. Furthermore, the laser facets are sensitive to accumulation of dust. Since the laser acts as optical tweezers, it sucks particles into regions with high intensities. Those particles can burn on the facets, destroying the anti-reflection coating and therefore deteriorating the diode. This doesn't happen very rapidly, but over several hundred hours of operation. Therefore, an enclosure that prevents dust from coming close to the diode should be used.

The diode should also be protected from current spikes and electrostatic discharges. If the diode is exposed, it will not necessarily die immediately, but may suffer minimal damage that can increase until the device stops working properly. Therefore, current drivers should include protection circuits to prevent the diode from experiencing transient currents, current spikes and reverse biases.

Back-reflections can also be very dangerous for the diode. They can degrade the

reflectivity of the facets and if a beam is reflected into the tapered area, it will focus and lead to an exceedingly high power density and damage the laser. Thus the optics should be slightly tilted.

Also, since the size of the chip is so small, a very large amount of heat in a small space is produced and a good connection to an adequate heatsink is an absolute must. For long operation times, the laser should be operated with a low temperature, since the lifetime depends exponentially on temperature.

Another thing to avoid is operating the amplifier with high currents and without the master laser coupled in over longer periods of time. If this occurs, most of the injected charge carriers will recombine in non-radiative processes, heating up the diode. Operating it with the injected beam over a longer period of time is not harmful.

III.10. Design Considerations for the Housing of the TA

The tapered amplifier chip (Sacher Lasertechnik - TPA-0780-1000) comes in a c-mount configuration. This assembly is then mounted to the copper block portion of the laser housing. One of the main design considerations for the housing is the high power of the TA. Since the TA also produces significant amount of heat and the frequency of the laser diode is very sensitive to temperature, heat transfer and control is a crucial feature. To keep the diode at the same temperature, the heat is conducted away through a large oxygen-free high conductivity (OFHC) copper block, in which the diode is mounted. Copper was chosen because it has low heat and

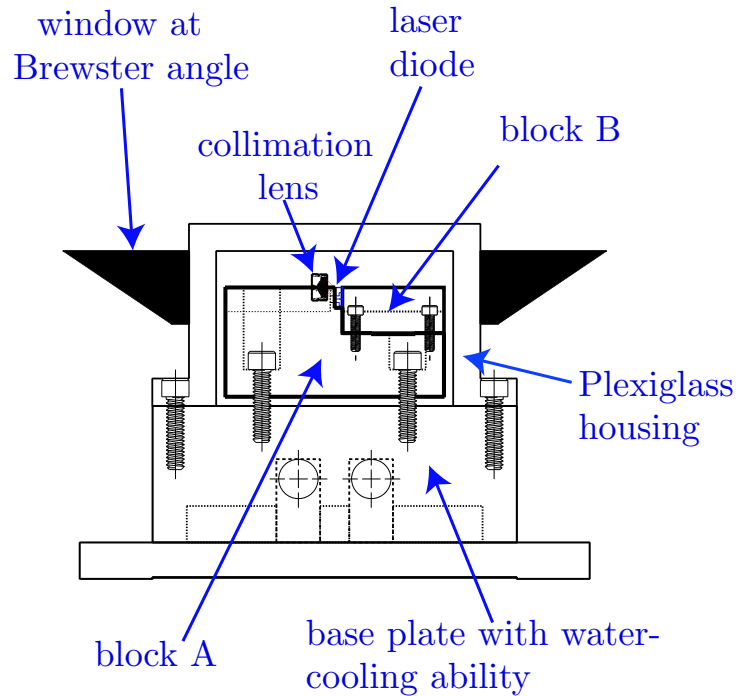


FIGURE III.6: Sideview of the tapered amplifier housing.

electrical resistance. The latter feature is important, because the mount of the laser diode acts as an anode and the driving current is conducted through the block. The heat is transferred via two thermo-electrical coolers (TEC, Melcor CP 1.0-127-05L) to an anodized aluminum block, which is the base of the entire housing. The baseplate is built to be water-cooled which turned out to be not necessary. The copper block is composed of three blocks bolted together. The diode is mounted to the largest block (see Fig. III.6, block A), which consists of two halves. The first is a flat base with a shallow channel milled (see the Appendix for drawings) through the middle, so that the other two copper pieces (fig. III.6, block B and block C, behind block B), which

are mounted to it, sit on the smallest possible surface and are therefore the least vertically tilted. The other half of this block is “v”-shaped. After the lens, attached to a translation stage as mentioned above, has reached its final position, two glass rods are slid between the lens and the “v” and the lens is glued down to those, which in turn are glued down to the block. Because of the v-shape, the rods can be moved up or down the v, which leads to a vertical degree of freedom for positioning the lens. A thin wall in the middle of the block separating the two halves is machined to be as flat and smooth as possible, then sanded and finished with 5 micron sandpaper in order to provide a good contact surface. The c-mount of the tapered amplifier is screwed to this wall and sits on a L-shaped bench, such that the actual chip is above the top of the wall but in maximal thermal contact with the surrounding copper. The top of the wall is cut at an angle in order to not clip the collimating beam.

The second piece (C) is also v-shaped and the output collimating lens is glued to it. When the collimation lenses are in the right position, the output lens blocks the access to the screw that bolts the diode to the wall. If the amplifier chip needs to be replaced, the v-block and therefore the lens can be removed and the diode can be removed. In order to get the new diode back in the right position, another small copper piece is bolted to the wall of the large block, joining the c-mount. The diode can simply be pressed against this piece and then tightened down. The third piece B bolted to the large block serves this same purpose of getting the v-block and therefore the output lens back into the correct position. The anode of the diode

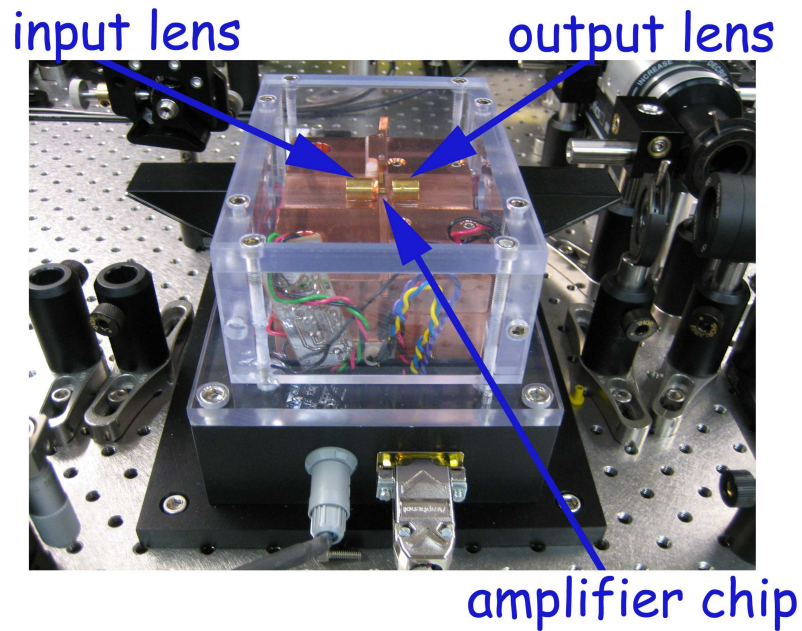


FIGURE III.7: Picture of the tapered amplifier housing.

is connected to the c-mount, so that electrical contact is established via the copper block. The cathode is connected by a lead bolted between two copper plates, which are in turn connected to the current supply. In order to protect the amplifier from the risk of being electrically damaged a protection circuit is put between the diode and the current supply, close to the diode.

A laser diode at room temperature can operate in about a range ± 30 K, but the lifetime depends strongly on the temperature, so cooling down the diode can noticeably enhance its lifetime. On the other hand, cooling down the diode to below 15°C can result in water condensation inside the laser housing. Furthermore, the diode should be in a dust free space. A polycarbonate housing with windows tilted at

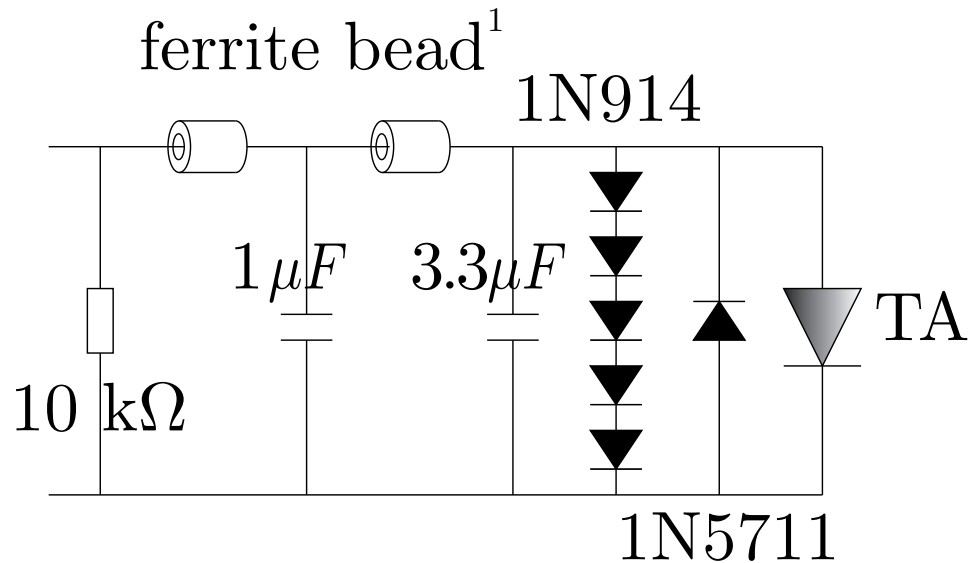


FIGURE III.8: Schematic of the protection circuit. The diodes prevent the TA from forward and backward transients, the ferrite bead and the capacitors form a low-pass filter. The ferrite beads (¹) are Panasonic EXC-ELSA 35.

the Brewster angle keeps the laser dust-free and prevents ambient air from warming up the copper block.

III.11. The Temperature Encounter

The temperature controller, like the current controller, is home-built. It was originally designed in Mark Raizen's lab at Austin and modified for our lab. Its function is to control the temperature of a master or a slave laser. The core of the board is the proportional-integral (PI) controller WTC3243 from Wavelength Electronics. Since the tapered amplifier uses much more current and has a higher power dissipation than the other lasers, the board had to be altered. For high diode currents, the error of the PI controller and the temperature of the diode kept increasing. Raising the

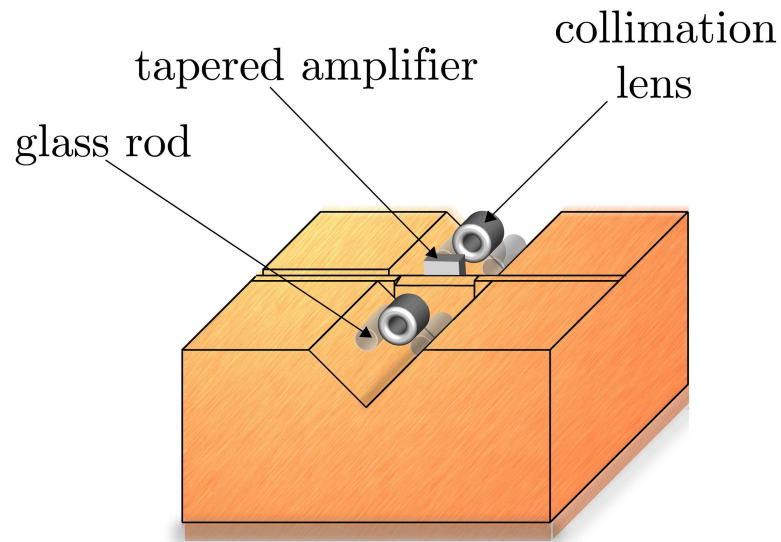


FIGURE III.9: Schematic drawing of the tapered amplifier housing.

TEC current limit at the PI-chip did not have an effect since the 5 V voltage of the supply was not high enough to drive sufficient current through the cooler. Therefore, the board was modified such that the chip could use a 15 V supply for the TEC current. But now the chip drew more than 2 A even without being connected to the TEC, in spite of the fact that the current was limited to 1.6 A. After desoldering the chip and exchanging it with a new one, the controller obeyed the 1.6 A current limit. However, for high laser powers, the TEC current would settle down and then slowly rise again along with the PI error. This problem was solved and the system stabilized by adding a second thermo-electric cooler. The problem with having only a single cooler is, that it pumps the heat to the baseplate where it cannot be dissipated quickly enough. Heat convects up to the cooled part again and raises the error which

raises the current, which in turn, heats up the TEC itself.

CHAPTER IV

Results

IV.1. Amplified Spontaneous Emission

If the diode is unseeded, it simply produces amplified spontaneous emission (ASE). The current dependency is shown in Fig. IV.1. Since the facets are reflect a small

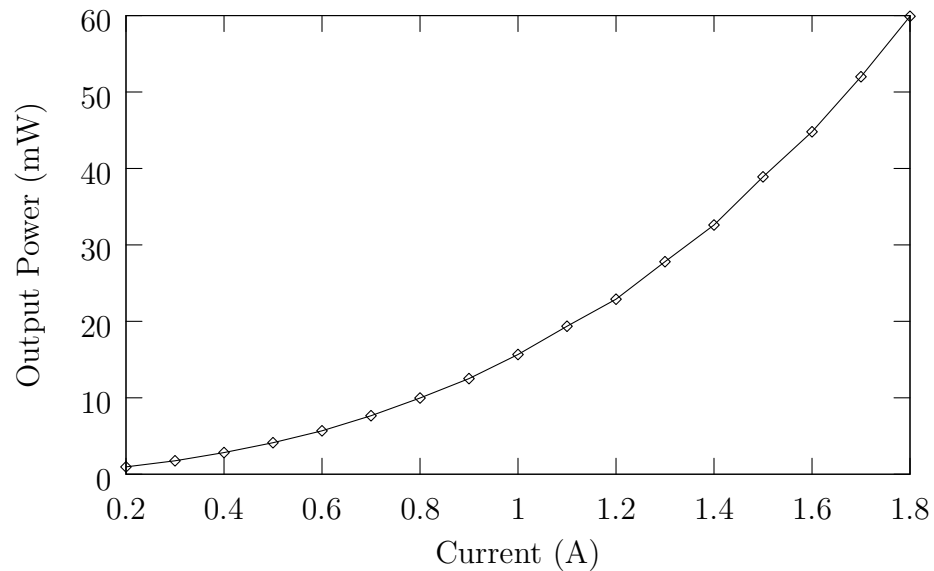


FIGURE IV.1: Horizontal beam profile of the amplified spontaneous emission at a current of $I_{TA} = 0.75A$, after the collimation and the cylindrical lens.

amount, the diode acts as a laser diode showing a threshold followed by a linear increase of power versus current. Fig. IV.2 shows a horizontal beam profile. The pro-

file was taken by scanning the power meter (Newport 1825-C with detector Newport 818-SL) with a $50 \mu\text{m}$ pinhole filter attached across the beam.

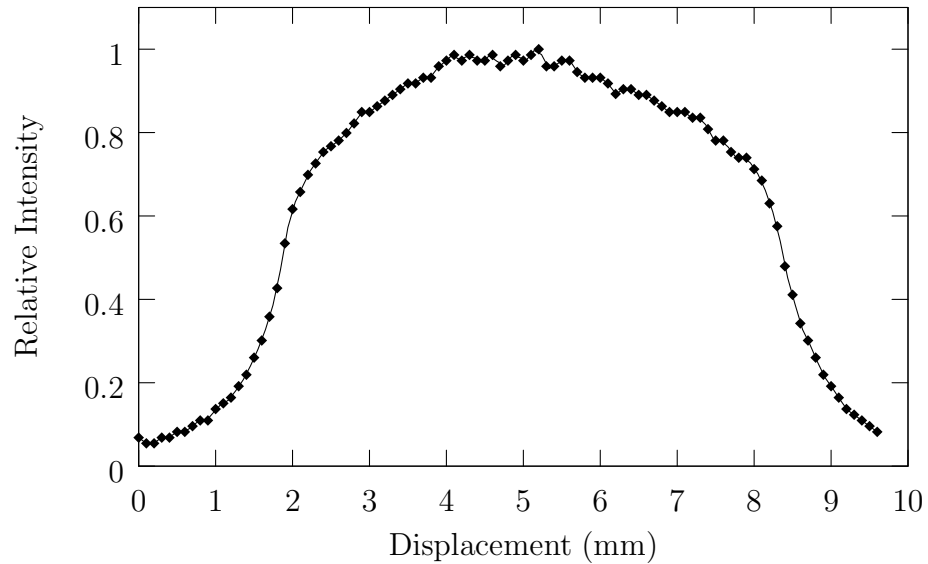


FIGURE IV.2: Horizontal beam profile of the amplified spontaneous emission at a current of $I_{TA} = 0.75A$, after the collimation and the cylindrical lens.

In Fig. IV.3, the broad frequency spectrum of the ASE can be seen.

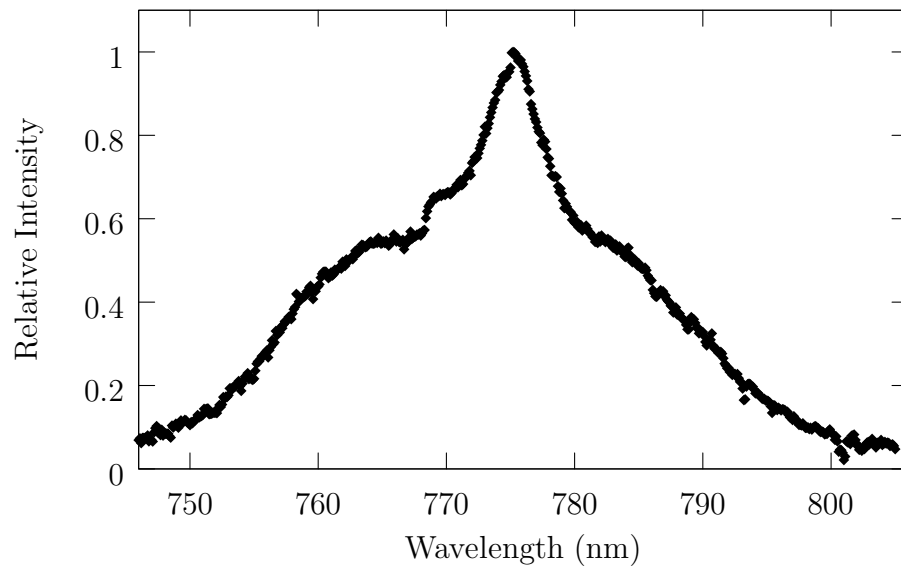


FIGURE IV.3: Low resolution ASE spectrum at $I_{TA} = 1.5A$ and $17.5\text{ }^{\circ}C$.

IV.2. Amplification of the Seed Beam

To determine the optimal seed power, the amplifier was operated at 2000 mA and the power of the input beam was varied. The output power increased very fast and quickly exceeded 1 W (Fig. IV.4). Another measurement with a current of 1600 mA was taken to prevent the facets from too high power densities. This measurement showed a saturation value of about 8 mW.

The current versus output power dependence for different temperatures is shown in Fig. IV.5. It can be seen that the power increases with lower temperatures (about 1.5 % per 1 K temperature change). It can also be seen that the amplification an 8 mW seed power is about 125. The power dependence of the tapered amplifier for

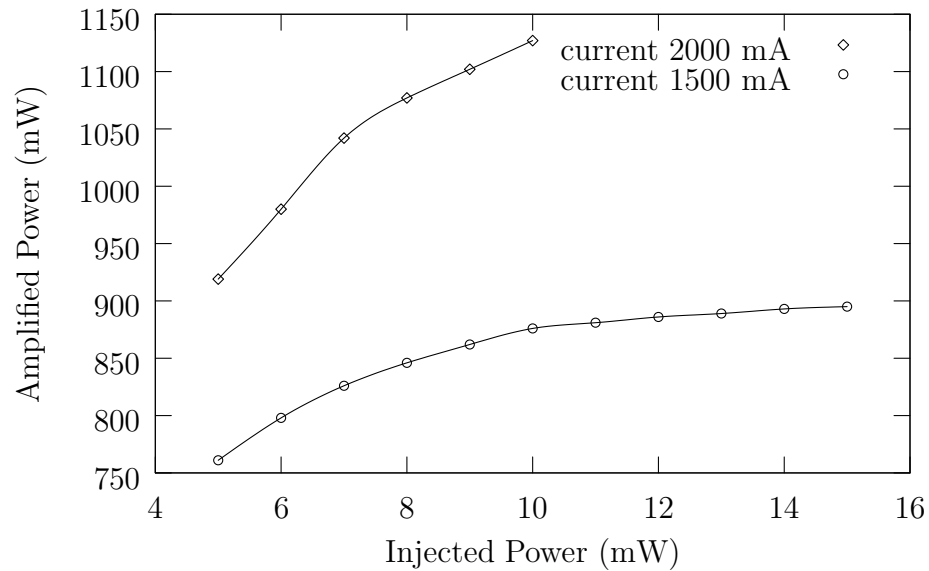


FIGURE IV.4: Power of the input laser versus the amplified power for two amplifier currents: 1600 mA and 2000 mA.

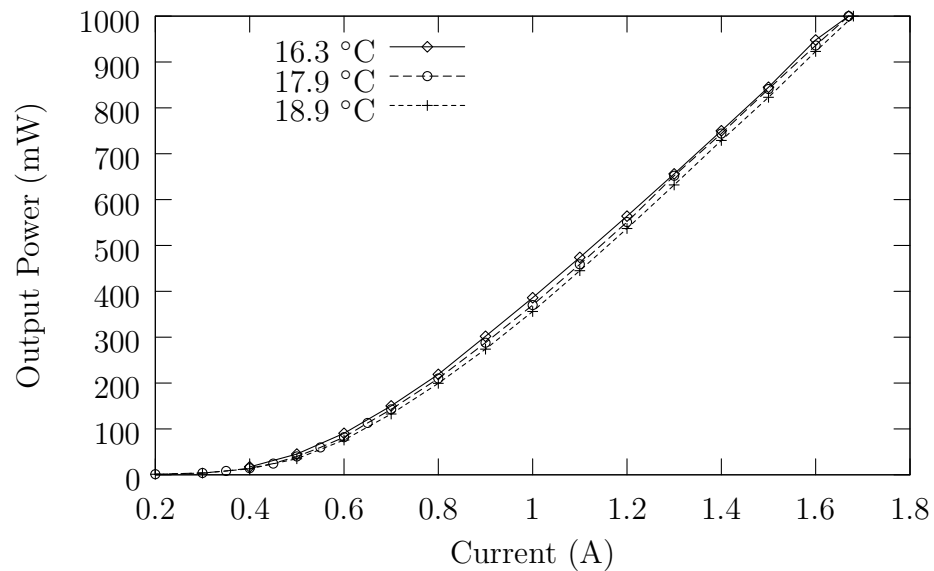


FIGURE IV.5: Temperature dependence of the output power versus the driving current.

different seeding powers can be seen in Fig. IV.6. The output power increases only slightly for currents above 8mW, since the amplifier is already saturated.

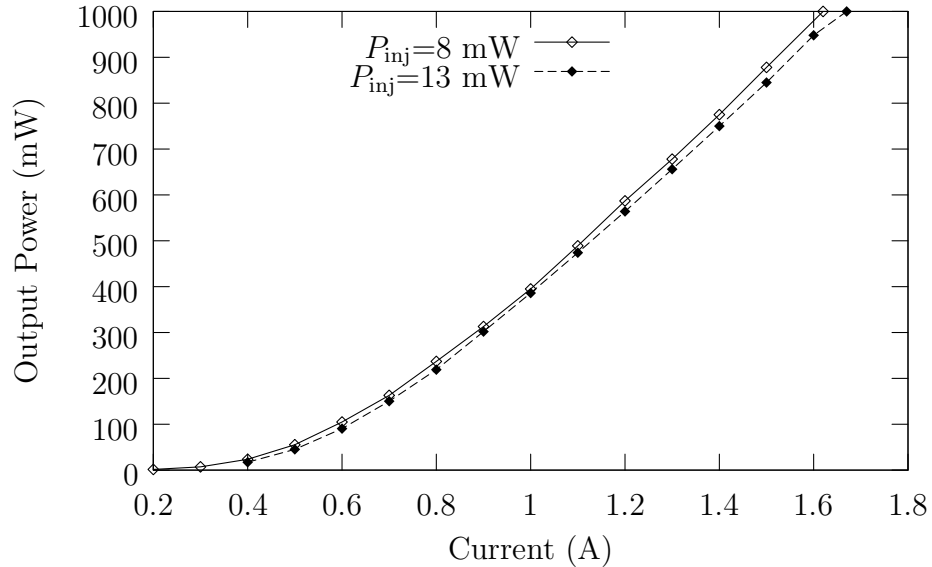


FIGURE IV.6: Output power versus current for two different seed powers of 8 mW and 13 mW.

IV.3. Spectrum

A spectrum was taken with a SA Instruments H20 monochromator. But since the input and output slits of the monochromator were missing, 100 μm pinholes were mounted both on the input aperture and in front of the power meter. The power meter was positioned directly after the output facet of the spectrometer. The drawback of this setup is that a constant-intensity background disturbs the signal, because the detection diode is not completely shielded against background light. Therefore, the ASE background is very hard to separate from the surrounding light entering the

photodiode.

IV.4. Optimizing the Output of the TA

To optimize the output of the laser, the optics were adjusted to yield the highest possible power and the spectrum was measured. Then the input optics were tweaked until the maximal power at 780 nm was achieved and the spectrum was measured again. Fig. IV.7 shows the two curves.

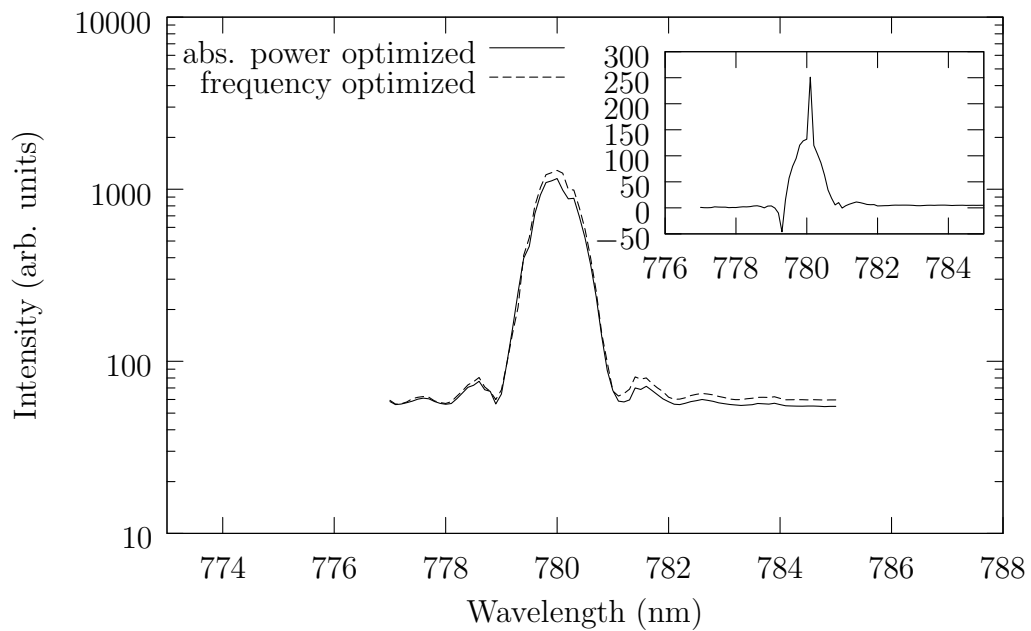


FIGURE IV.7: Spectrum of the TA for a output power of 0.5 W. The solid curve is optimized for the most absolute power, the dashed curve for the most power at 780 nm. The inlet shows the difference between both graphs. Note: the inlet has a linear y-axis.

Since the peak of the output beam moves a very small spatial amount after the input optics are adjusted, the absolute difference of the peaks and of the spectral

backgrounds is not very meaningful. But one can get rid of the intensity background by taking the difference of the curves and obtain information about the improvement. For the difference spectrum, the ratio of the ASE background to the peak intensity is 18.6%. Therefore, the power in the peak can be slightly increased by maximizing the intensity at the central frequency. This can also be seen in the ratios of the ASE to peak intensity. The intensities were obtained by calculating the integral of the spectral power densities. The lower boundary was obtained by subtracting the lowest measured value from the data, approximating the background as a constant offset. The upper boundary was obtained by dividing the integral by the number of measurement points, getting an averaged spectral power density for both, the peak and the ASE. For the absolute intensity-maximized beam this ratio is 2.7% – 11.4% and for the beam, maximized at 779.9 nm, it is 3.6% – 10.5%. These values are in agreement with [17], measuring 5.6% of the total intensity in the peak.

IV.5. Spatial Profile

The following section describes the spatial properties of the beam. The beam will eventually be coupled into a single-mode fiber. Therefore, a Gaussian-like spatial distribution is desirable to get a high coupling efficiency. The spatial profile is measured after the optical isolators, by measuring the power transmitted through a pinhole translated across the beam. Fig. IV.8 shows the horizontal profile, a distribution along the x-axis in Fig. V.1 compared to a fitted Gaussian function. One has to con-

sider that a phase-sensitive measurement is needed for a quantitative characterization of the beam quality. The vertical profile is depicted in fig. (IV.9).

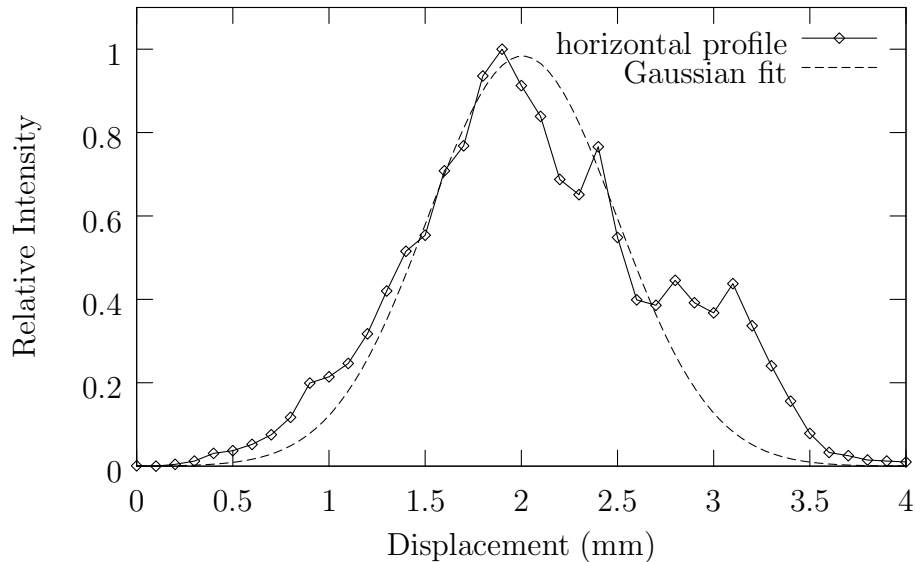


FIGURE IV.8: Horizontal profile for a seeding laser power of $P_{seed} = 8$ mW and an amplifier power of $P_{TA} = 100$ mW.

To observe the response of the beam for different parameters, the power of the TA and the seed power has been changed. In Fig. IV.10 and Fig. IV.11, the power of the amplifier has been changed, whereas the input power was the same. It can be seen that the beam shape becomes slightly smaller for higher powers. This is expected because for higher powers, more intensity is in the central lobe and the amplified spontaneous emission, which is spatially displaced from the center becomes relatively smaller.

In curves in Fig. IV.12 and Fig. IV.13 show the beam for the same amplifier power but for a different seeding power. For the seeding power of $P_{seed} = 13$ mW,

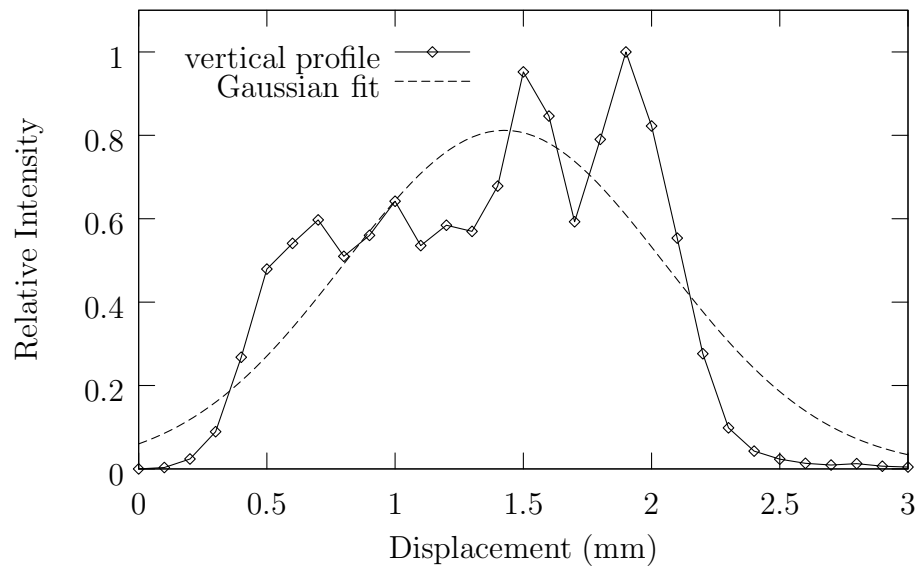


FIGURE IV.9: Vertical profile for a seeding laser power of $P_{\text{seed}} = 8$ mW and an amplifier power of $P_{\text{TA}} = 100$ mW.

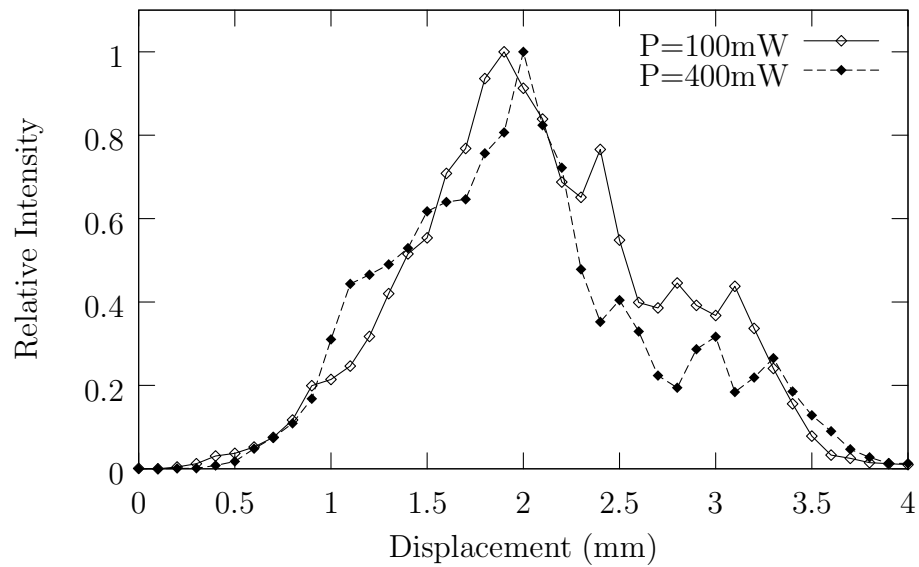


FIGURE IV.10: Horizontal profile of the TA for the same input power of 8 mW and an output power of the tapered amplifier of 100 mW and 400 mW.

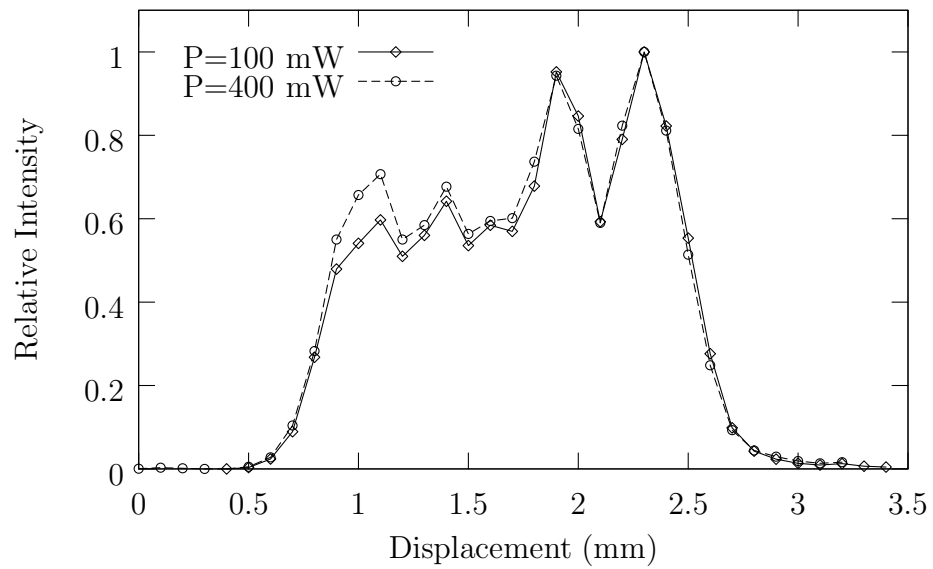


FIGURE IV.11: Vertical profile of the TA for the same input power of 8 mW and an output power of the tapered amplifier of 100 mW and 400 mW.

the horizontal beam profile becomes noticeably broader and less Gaussian-shaped.

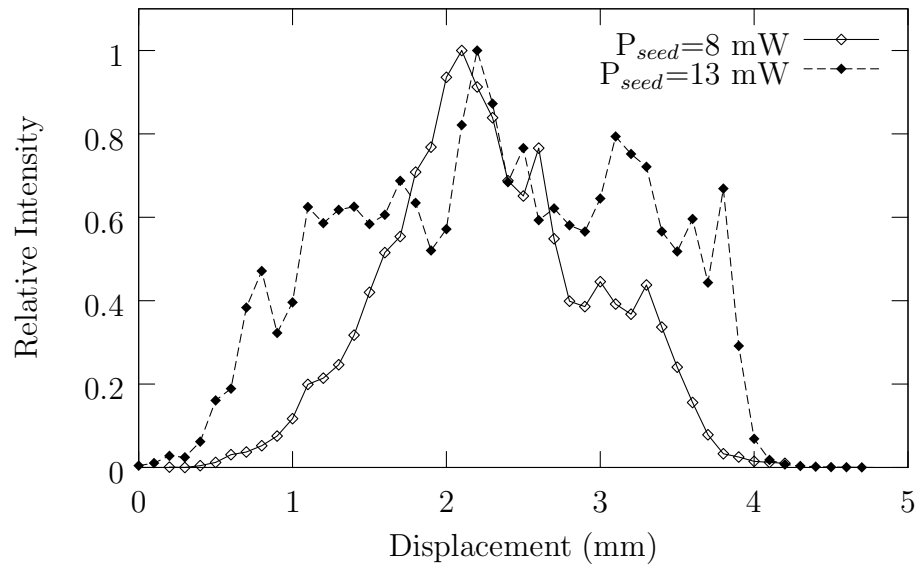


FIGURE IV.12: Horizontal beam profile for different input powers at the same output power of 100 mW.

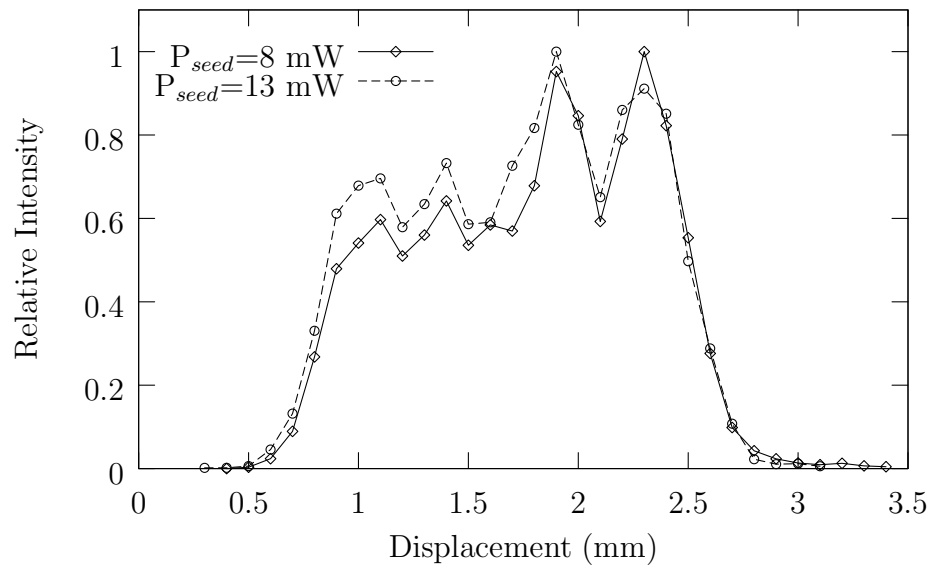


FIGURE IV.13: Vertical beam profile for different input powers at the same output power of 100 mW.

CHAPTER V

Conclusions

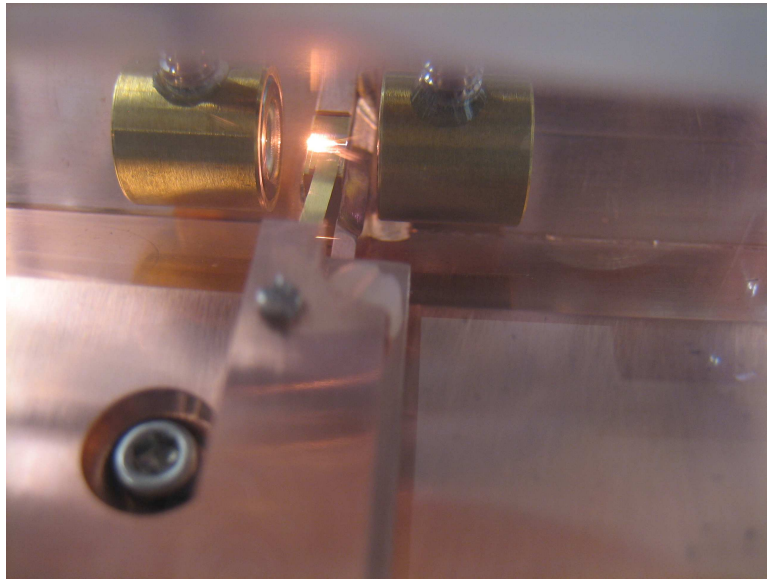


FIGURE V.1: Picture of the tapered amplifier, emitting to the left, with the two collimation lenses.

This thesis describes the development and setup of a home-build high power stabilized diode laser system. The system has the purpose of realizing a dipole trap for trapping ultracold rubidium atoms.

The system consists of the two major components: a master-slave laser setup that produces a narrow output with a frequency deviation of < 5 MHz. This beam is amplified by a tapered amplifier chip conserving a narrow spectrum. The output power of the system is 1 W of single-mode laser light.

The spatial and spectral properties of the single mode output beam of the tapered amplifier have been measured.

To further improve the beam quality, the beam will be coupled into a single mode fiber, which acts as a spatial and a spectral filter. A coupling efficiency of up to 60% has been reported [14].

APPENDIX A

Technical Drawings

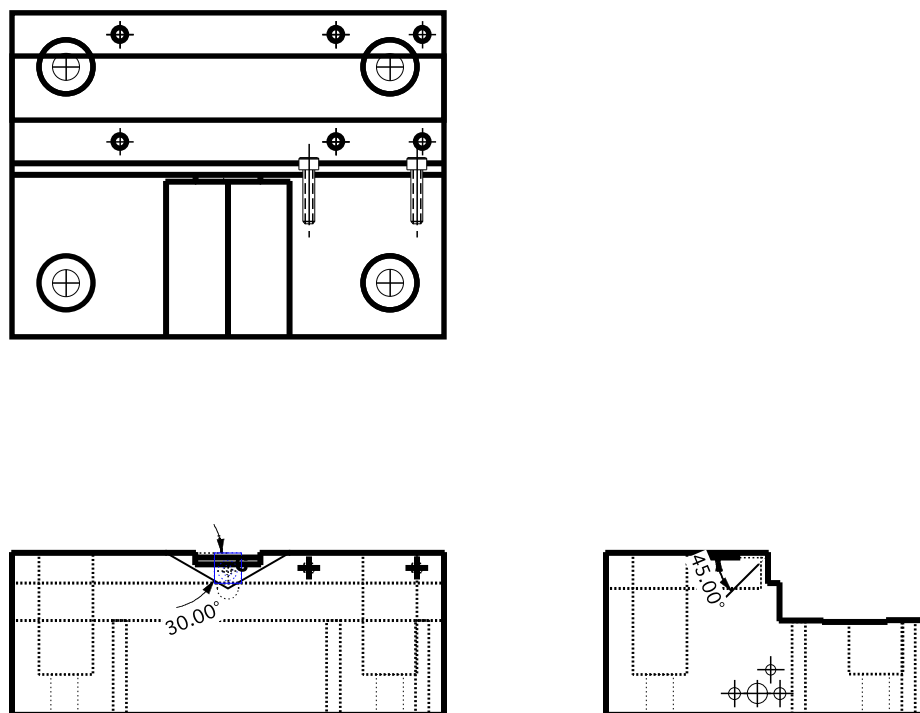


FIGURE A.1: Drawing of the large copper block (A).

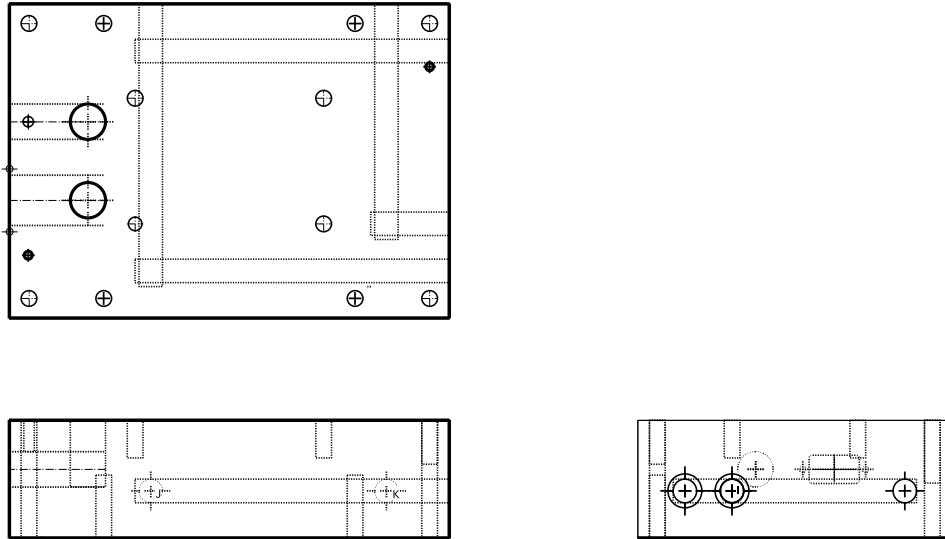


FIGURE A.2: Drawing of the baseplate with water-cooling ability.

BIBLIOGRAPHY

- [1] HAROLD J. METCALF, PETER VAN DER STRATEN, *Laser Cooling and Trapping* Springer-Verlag, 1999.
- [2] RODNEY LOUDON, *The Quantum Theory of Light* Oxford University Press, 1983.
- [3] R. DIEHL (ED.), *High-Power Diode Lasers* Springer-Verlag, 2000.
- [4] BRIAN DEMARCO, *Quantum Behavior of an Atomic Fermi Gas* Ph.D. Thesis, University of Colorado - Boulder, 2001.
- [5] J.N. WALPOLE, *Semiconductor amplifiers and lasers with tapered gain region* Opt. Quantum Electron, 28, 1996, 623-645.
- [6] CARL E. WIEMAN, LEO HOLLBERG, *Using diode lasers for atomic physics* Rev. Sci. Instrum. 62 (1), January 1991.
- [7] DEMTRÖDER, *Experimentalphysik 3* Springer Verlag, 2000.
- [8] D. MESCHEDE, *Gerthsen Physik* Springer Verlag, 2002.
- [9] W.W. CHOW, S.W. KOCH, *Semiconductor-Laser Fundamentals* Springer Verlag, 1999.
- [10] E. HECHT, *Optics* Addison Wesley, 1998.
- [11] J.N. WALPOLE, E.S. KINTZER, S.R. CHINN, C.A. WANG, AND L.J. MIS-SAGGI, *Appl. Phys. Lett.* **61** , 740 (1992).
- [12] B.SUMPF G.BEISTER, G.ERBERT, J.FRICKE, A.KNAUER, P.RESEL, AND G. TRÄNKLE, "Reliable 1-W CW Operation of High-Brightness Tapered Diode Lasers at 735nm" *IEEE Photon. Technol. Lett.*, vol. **16**, 984-986 (2004).
- [13] S. SUJECKI, L. BORRUEL, J. WYKES, P. MORENO, B. SUMPF, P. SEWELL, H. WENZEL, T. M. BENSON, G. ERBERT, I. ESQUIVIAS, E. C. LARKINS, "Nonlinear Properties of Tapered Laser Cavities" *IEEE J. Select. Topics Quant. Electr.*, **9**, 3, 823 (2003).

- [14] R. A. NYMAN, G. VAROQUAUX, B. VILLIER, D. SACCHET, F. MORON, Y. LECOQ, A. ASPECT, P. BOUYER, “Tapered-amplified AR-coated laser diodes for Potassium and Rubidium atomic-physics experiments. ” *Review of Scientific Instruments* **77**, 033105 (2006)
- [15] DANIEL A. STECK, “QUANTUM CHAOS, TRANSPORT, AND DECOHERENCE IN ATOM OPTICS” *Ph.D. Thesis, University of Texas, Austin 2001*.
- [16] BRUCE G. KLAPPAUF, “EXPERIMENTAL STUDIES OF QUANTUM CHAOS WITH TRAPPED CESIUM” *Ph.D. Thesis, University of Texas, Austin 1998*.
- [17] DIRK VOIGT, “Evanescent-Wave Mirrors for Cold Atoms” *Ph.D. Thesis, Universiteit van Amsterdam 2000*.
- [18] J.-PH. BOUYER, CH. BRÉANT , “Stability of an injection-locked DFB 1.5 μm semiconductor laser ” *J. Phys. III France 2 (1992) 1623-1644*.
- [19] Datasheet Sacher Laser